

1  
2  
3  
4  
5  
6  
7  
8  
9  
10  
11  
12  
13  
14  
15  
16  
17  
18  
19  
20  
21  
22  
23  
24  
25  
26  
27  
28  
29  
30

***Schistosoma mansoni* immunomodulatory molecule Sm16/SPO-1/SmSLP is a member of the trematode-specific helminth defence molecules (HDMs)**

Jenna Shiels<sup>1,2</sup>, Krystyna Cwiklinski<sup>1,3</sup> Raquel Alvarado<sup>4</sup>, Karine Thivierge<sup>5,^</sup>, Sophie Cotton<sup>5</sup>, Bibiana Gonzales Santana<sup>5</sup>, Joyce To<sup>4</sup>, Sheila Donnelly<sup>4</sup>, Clifford C. Taggart<sup>2</sup>, Sinead Weldon<sup>2</sup>, and John P. Dalton<sup>1,3,5</sup>

<sup>1</sup> School of Biological Sciences, Queen’s University Belfast, Northern Ireland

<sup>2</sup> Airway Innate Immunity Group (AiiR), Wellcome Wolfson Institute for Experimental Medicine (WWIEM), School of Medicine, Dentistry and Biomedical Sciences, Queen’s University Belfast, Northern Ireland.

<sup>3</sup> Center of One Health (COH) and Ryan Institute, School of Natural Science, National University of Ireland Galway, Galway, Ireland.

<sup>4</sup> School of Life Sciences, Faculty of Science, The University of Technology Sydney, Ultimo, NSW, Australia.

<sup>5</sup> Institute of Parasitology, McGill University, Montreal, Quebec, Canada.

<sup>^</sup>Present address: Laboratoire de Santé Publique du Québec, Institut National de Santé Publique du Québec, 20045, Chemin Sainte-Marie, Sainte-Anne-de-Bellevue, Québec, Canada H9X 3R5.

\*Correspondence to: johnpius.dalton@nuigalway.ie

**Keywords:** *Schistosoma*; Fasciola; helminth; trematode; parasite; Sm16; SPO-1; SmSLP; helminth defence molecule; immunomodulation, PPAR/LXR.

31

32 **ABSTRACT**

33 **Background-** Sm16, also known as SPO-1 and SmSLP, is a low molecular weight protein  
34 (~16kDa) secreted by the digenean trematode parasite *Schistosoma mansoni*, one of the main  
35 causative agents of human schistosomiasis. The molecule is secreted from the acetabular  
36 gland of the cercariae during skin invasion and is believed to perform an immune-suppressive  
37 function to protect the invading parasite from innate immune cell attack.

38 **Methodology/Principal Findings-** We show that Sm16 homologues of the  
39 Schistosomatoidea family are phylogenetically related to the helminth defence molecule  
40 (HDM) family of immunomodulatory peptides first described in *Fasciola hepatica*.  
41 Interrogation of 69 helminths genomes demonstrates that HDMs are exclusive to trematode  
42 species. Structural analyses of Sm16 shows that it consists predominantly of an amphipathic  
43 alpha-helix, much like other HDMs. In *S. mansoni*, Sm16 is highly expressed in the cercariae  
44 and eggs but not in adult worms, suggesting that the molecule is of importance not only  
45 during skin invasion but also in the pro-inflammatory response to eggs in the liver tissues.  
46 Recombinant Sm16 and a synthetic form, Sm16 (34-117), bind to macrophages and are  
47 internalised into the endosomal/lysosomal system. Sm16 (34-117) elicited a weak pro-  
48 inflammatory response in macrophages *in vitro* but also suppressed the production of  
49 bacterial lipopolysaccharide (LPS)-induced inflammatory cytokines. Evaluation of the  
50 transcriptome of human macrophages treated with a synthetic Sm16 (34-117) demonstrates  
51 that the peptide exerts significant immunomodulatory effects alone, as well as in the presence  
52 of LPS. Pathways most significantly influenced by Sm16 (34-117) were those involving  
53 transcription factors peroxisome proliferator-activated receptor (PPAR) and liver X  
54 receptors/retinoid X receptor (LXR/RXR) which are intricately involved in regulating the  
55 cellular metabolism of macrophages (fatty acid, cholesterol and glucose homeostasis) and are  
56 central to inflammatory responses.

57 **Conclusions/Significance-** These results offer new insights into the structure and function of  
58 a well-known immunomodulatory molecule, Sm16, and places it within a wider family of  
59 trematode-specific small molecule HDM immune-modulators with immuno-biotherapeutic  
60 possibilities.

61

62

63 **AUTHOR SUMMARY**

64 Sm16 is a low molecular weight protein (~16kDa) secreted by *Schistosoma mansoni*, a  
65 causative agent of human schistosomiasis. The molecule is secreted by the infectious  
66 cercariae during skin invasion and performs an immune-suppressive function to protect the  
67 invading parasite from immune attack. Using phylogenetic and gene structure analysis we  
68 show that Sm16 homologues of parasites belonging to the Schistosomatoidea superfamily of  
69 digenean worms are members of the helminth defence molecule (HDM) family that are  
70 potent immune-modulators and exclusive to trematode species. Structural analyses revealed  
71 that Sm16, much like other HDMs, consists predominantly of an amphipathic alpha-helix.  
72 Sm16 is highly expressed in the cercariae and eggs of *S. mansoni* but not male or female  
73 adult worms, suggesting that the molecule is of importance not only during skin invasion but  
74 also in the pro-inflammatory response to eggs in the liver tissues. A synthetic form of the  
75 molecule, termed Sm16 (34-117), was shown to bind to and enter immune cells  
76 (macrophages) and induce a weak pro-inflammatory response. However, this peptide also  
77 blocked the pro-inflammatory effects of bacterial endotoxin (lipopolysaccharide, LPS).  
78 Analysis of the transcriptome of Sm16 (34-117)-stimulated macrophages in the presence or  
79 absence of LPS suggests that it mediates immunomodulatory activity via signalling pathways  
80 that are intricately involved in regulating cellular metabolism (fatty acid, cholesterol and  
81 glucose homeostasis) and central to inflammatory responses. These new insights into the  
82 structure and function of a well-known immunomodulatory molecule, Sm16, places it within  
83 a wider family of trematode-specific small molecule HDM immune-modulators with  
84 immuno-biotherapeutic possibilities.

85

86

87 **INTRODUCTION**

88 Human schistosomiasis is a public health issue affecting approximately 200 million people in  
89 over 74 tropical/sub-tropical countries, with many more people at risk of infection [1]. The  
90 causative pathogens are digenean trematode parasites of the genus *Schistosoma*, mainly  
91 *Schistosoma mansoni*, *S. japonicum* and *S. haematobium*. Chronic schistosomiasis has a  
92 significant impact on morbidity and mortality as it affects the immune system, fertility,  
93 growth, and development throughout life [2].

94

95 Schistosomiasis is acquired by contact with water containing free-swimming schistosome  
96 larvae, cercariae, that attach to and penetrate the skin. Itching or a rash on the skin can occur  
97 at the parasite's point of entry. After a period of migration in the host, the worms mature to  
98 adults and reside as male-female pairs either in mesenteric venules (*S. mansoni* and *S.*  
99 *japonicum*) or in the venous plexus of the bladder (*S. haematobium*), where they produce  
100 approximately 300 (*S. mansoni*) to 3,500 (*S. japonicum*) eggs per day [3]. Eggs are passed  
101 through blood vessels and the wall of the digestive tract or the urinary bladder, where they  
102 are subsequently passed in faeces or urine into the environment. However, eggs can become  
103 lodged in intestinal or bladder tissue, and quite often the blood flow can displace the eggs and  
104 carry them to the liver where they become lodged in the tissue.

105

106 Typically, a weak Th1-type response is observed during the initial stages of schistosomiasis  
107 before there is a shift towards a Th2-type response concurrent with the deposition of eggs in  
108 the tissues. Schistosome eggs are highly immunogenic and release soluble antigens (SEA)  
109 that can directly modulate antigen presenting cells and promote Th2-dominant responses, an  
110 immune environment that is key to the survival of adult parasites that evade expulsion for up  
111 to 40 years [3-5]. Egg-induced granulomas consisting of a mass of cells, mainly eosinophils,  
112 Th2-type CD4<sup>+</sup> T-cells, and M2 macrophages, encapsulate the eggs [6,7]. While formation of  
113 granulomas is considered a protective mechanism to prevent excessive damage to host tissue,  
114 resolution of granulomatous tissue can cause considerable tissue fibrosis, particularly in cases  
115 of repeated and chronic infections [4,8].

116

117 Sm16 is a low molecular weight protein (~16 kDa) with immunomodulatory properties that is  
118 secreted by *S. mansoni* cercariae as they penetrate the host skin. Sm16 expression has been

119 described as stage-specific, with early reports indicating that it is expressed exclusively by  
120 sporocysts, cercariae, and early schistosomulae of *S. mansoni* [9,10]. Developmental  
121 expression analysis of *S. japonicum* suggested that the Sm16 homolog, Sj16, is enriched in  
122 eggs, miracidia, sporocysts, cercariae, and lung stage schistosomulae [11]. Recently,  
123 however, Bernardes et al. [12] reported that Sm16 is expressed in cercariae and newly  
124 transformed schistosomulae but not in adults or eggs.

125

126 Sm16 inhibits TLR-3 and TLR-4 signalling in human monocytes [13] and the activation of  
127 macrophages *in vitro* [14] and suppresses leukocyte accumulation when administered to mice  
128 [15-17]. Sj16 peptide can inhibit lipopolysaccharide (LPS)-induced nitric oxide production  
129 by macrophages, block macrophage phagocytic and migratory activity, and dendritic cell  
130 maturation [18-20]. It has also been reported to induce IFN- $\gamma$  and IL-10 secreting CD4+  
131 CD25+ Foxp3+ regulatory T cell (Treg) populations both *in vitro* and *in vivo* [21]. This  
132 immunomodulatory activity of Sm16/Sj16 has shown promise as an anti-inflammatory  
133 therapy by suppressing cutaneous inflammation when administered intra-dermally [17],  
134 reducing the severity of Freund's-induced arthritis in rats [22] and protecting against  
135 inflammatory colitis in a murine dextran sodium sulphite (DSS) model [23].

136

137 We have previously described a family of immunomodulatory molecules found in medically  
138 important flatworms such as *Fasciola hepatica* which we termed helminth defence molecules  
139 (HDMs) [24]. We showed that *F. hepatica* HDM (FhHDM-1) exhibits potent anti-  
140 inflammatory properties; for example, it suppresses leukocyte accumulation and ameliorates  
141 inflammatory disease in pre-clinical murine models of type 1 diabetes and multiple sclerosis  
142 [25,26]. Here we describe phylogenetic, structural and functional links between Sm16 and  
143 HDM-like molecules and show that expression of these molecules is exclusive to trematode  
144 parasites. Our analysis verifies the expression of Sm16 in *S. mansoni* cercariae and eggs but  
145 not in adult male or female worms. We show that the C-terminal section of Sm16 is  
146 predominantly an uninterrupted amphiphilic  $\alpha$ -helix that may allow the peptide to penetrate  
147 cells and enter the endosomal/lysosomal system of macrophages. Sm16 activates various  
148 inflammatory responses in macrophages, but also has potent inhibitory activity against LPS-  
149 induced inflammatory effects. RNA microarray and Ingenuity Pathway Analysis (IPA)  
150 predicted that several signalling pathways are affected by Sm16, most notably those

151 involving transcription factors, peroxisome proliferator-activated receptor (PPAR) and liver  
152 X receptors/retinoid X receptor (LXR/RXR), which are involved in regulating the cellular  
153 metabolism of macrophages and central to controlling inflammatory responses. Our findings  
154 provide valuable new insights into the role of Sm16 in host-parasite interactions at key stages  
155 of the schistosome life-cycle and place it amongst the wider family of trematode-specific  
156 small molecule HDM immune-modulators that have potential in the development of novel  
157 immuno-biotherapeutics.

158

159

## 160 **MATERIALS AND METHODS**

### 161 **Preparation of *S. mansoni* samples**

162 *S. mansoni* cercariae and livers from infected mice were a gift from the laboratory of Dr.  
163 Paula Ribeiro, McGill University. Mature *S. mansoni* were recovered from the mesenteric  
164 veins of infected mice (kindly provided by the Biomedical Research Institute, Rockville,  
165 Maryland, USA). Worms were transferred into DMEM for one to two hours at 37°C until the  
166 adult male and female were separated. Males and females were conserved separately at -80°C  
167 for protein extraction or in RNAlater (Ambion) for RNA extraction. Eggs were isolated from  
168 livers according to the procedure of Dalton et al. [27]. Infected mouse livers were also cut  
169 into small cubes and fixed in 4% paraformaldehyde in preparation for immunolocalization  
170 (see below). Serum was prepared from blood taken from mice infected with 35 cercariae at  
171 5-, 10- and 20-weeks post-infection. Animal procedures were reviewed and approved by the  
172 Facility Animal Care Committee of McGill University and were conducted in accordance  
173 with the guidelines of the Canadian Council on Animal Care.

174

175 Proteins were extracted from cercariae, eggs, adult males and adult females with 200 µL of  
176 PBS pH 6.8 containing proteinase inhibitor cocktail (1 tablet/10ml; Roche, USA) using a pre-  
177 chilled Dounce homogenizer. Mixtures were submitted to three freeze-thaw cycles in a  
178 freezer set to maintain -20°C. Total proteins were recovered by centrifuging 30 minutes at  
179 17,900 x g in a conventional tabletop microcentrifuge at 4°C. Protein concentrations were  
180 evaluated by Bradford assay.

181

182 **Production of Sm16 by recombinant expression and chemical synthesis**

183 Recombinant Sm16 was produced in *Pichia pastoris* using the method previously described  
184 in Collins et al. [28]. The recombinant protein (residues 23-117, which excluded the signal  
185 sequence) was produced by fermentation at 30°C and 250-300 rpm in one litre BMGY broth  
186 buffered to pH 6.0 into 4 litre baffled flasks until an OD<sub>600</sub> of 2-6 was reached. The cells  
187 were centrifuged at 3,000 x g for 10 minutes at room temperature and the induction initiated  
188 by resuspending the pellets in 200 ml BMMY broth and adding 1% filter-sterilized methanol  
189 every 24 hours for 3 days. The culture was then centrifuged at 16,000 x g for 30 minutes at  
190 RT. The pellets were discarded and Sm16 was isolated from the supernatant by Ni-NTA  
191 affinity chromatography. Recombinant *S. mansoni* cathepsin B1 (SmCB1) was produced in a  
192 similar manner as reported by Stack et al. [29].

193 A synthetic peptide corresponding to residues 34 to 117 of Sm16 (34-117) and  
194 various derivatives of this peptide were synthesised upon request by GL Biochem (Shanghai,  
195 China) and was dissolved in sterile, endotoxin-free water (Sigma Aldrich, UK) at 1 mg/ml  
196 and stored aliquoted at -80°C.

197

198 **Anti-Sm16 antibodies.**

199 Polyclonal antibodies were produced in rabbits against the peptide sequence  
200 'MDKYIRKEDLGMKMLDVAKILGRRIEKRMEYIAKKC' of Sm16 by Genscript (New  
201 Jersey, USA). The cysteine was added to the C-terminus to facilitate conjugation to  
202 ovalbumin. Antibodies were lyophilized prior to shipping and were resuspended in ultrapure  
203 water before the specific anti-Sm16 peptide antibody was purified by immune-affinity  
204 chromatography. The Sm16 peptides were covalently immobilized to a beaded agarose  
205 support using the SulfoLink Immobilization kit for peptides following the manufacturer's  
206 recommendations (Thermo Scientific, USA).

207

208 **Phylogenetic analyses**

209 Homologous sequences were identified by TBLASTN analysis of the publically available  
210 genome databases at WormBase ParaSite (<http://parasite.wormbase.org/index.html>.  
211 Version: WBPS11) from 42 species of the phylum Nematoda and 27 species of phylum  
212 Platyhelminthes (S1 Table; S2 Table). BLAST analysis was based on the *F. hepatica* HDM

213 sequence (CCA61804) and the *S. mansoni* Sm16 sequence (AAD26122), in addition to  
214 previously characterised HDM and Sm16 sequences from *Clonorchis sinensis*,  
215 *Opisthorchis viverrini* and *Schistosoma* spp (S1 Table; S2 Table). Inclusion criteria for  
216 phylogenetic analysis were based on primary sequence alignments and confirmation of an  
217 amphipathic helix by helical wheel projections (HeliQuest). Protein alignments were carried  
218 out using MAFFT using the ginsi options [30], which was hand-edited using Geneious  
219 (v11.1.5; <https://www.geneious.com>) resulting in a contiguous sequence block ranging  
220 from Leu<sup>30</sup> to Lys<sup>87</sup> (FhHDM nomenclature) containing the amphipathic region of the  
221 proteins. Phylogenetic trees were constructed with PhyML 3.0 [31] using the phylogenetic  
222 model LG +G+I, with five random starting trees and 1000 bootstrap support. The final tree  
223 figures were generated using FigTree (<http://tree.bio.ed.ac.uk/software/figtree/>).

224

## 225 **Structural analyses**

226 The signal peptide at the N-terminus of Sm16 was identified using the SignalP 4.1 server  
227 [32]. The amino acid sequence of Sm16 was entered into the I-TASSER server (accessible  
228 via. <https://zhanglab.ccmb.med.umich.edu/I-TASSER/>) to obtain an *ab initio* prediction of  
229 the secondary structure. The I-TASSER server was also used to obtain a putative 3D model  
230 of secreted Sm16 [33]. The HeliQuest tool [34], was used to construct helical wheel  
231 projections. Circular dichroism (CD) spectra of recombinant Sm16 were recorded using a  
232 Jasco J-815 CD spectropolarimeter. Wavelength scans were performed between 190 and 250  
233 nm in 10 mM Tris, 50 mM NaF buffer (pH 7.3) in both the presence and absence of  
234 trifluoroacetic acid (TFE) [30% and 60% (v/v)] with a sample concentration of 100 µg/ml.  
235 Spectra were recorded in a 1 mm quartz cuvette at 20°C. Data below 190 nm for the native  
236 Sm16 sample were removed from analyses due to low signal-to-noise.

237

## 238 **Cell culture**

239 The human acute monocytic leukaemia THP-1 cell line (ATCC, Manassas, USA) was  
240 routinely cultured (P2-30) in RPMI 1640 medium with L-glutamine (2 mM) (Gibco,  
241 ThermoFisher Scientific, UK) supplemented with 10% (v/v) heat-inactivated foetal calf  
242 serum (FCS; Gibco, ThermoFisher Scientific, UK) and 1% (v/v) penicillin/streptomycin  
243 (PAA Laboratories GmbH, Pasching, Austria). Cells were seeded at a density of  $2.5 \times 10^5$



244 cells/well in 24 well plates and were differentiated to macrophages by incubating with 2 ml  
245 of medium with 162 nM phorbol 12-myristate 13-acetate (PMA; Sigma Aldrich, UK) for 72  
246 hrs, then rested in fresh media (PMA-free) for 24 hrs before use. Cells were incubated with  
247 peptides (20 µg/ml) and/or LPS from *Pseudomonas aeruginosa* (100 ng/ml, Serotype 10,  
248 Source strain ATCC 27316; Sigma Aldrich, UK) in media for 16 hrs.

249

### 250 **Isolation and culture of bone marrow derived macrophages (BMDM)**

251 Bone marrow was harvested from C57BL/6 and Balb/c mice and differentiated into  
252 macrophages over 6 days in RPMI medium supplemented with 10% FCS,  
253 penicillin/streptomycin (100 U/ml), L-Glutamine (2 mM), 2-mercaptoethanol (2-ME; 50 µM)  
254 and macrophage colony-stimulating factor (M-CSF; 50 ng/ml; eBiosciences). For  
255 experimentation, cells were counted by trypan blue exclusion, seeded at a density of 1.25 x  
256 10<sup>5</sup> cells/well, and left to adhere overnight. Cells were stimulated in fresh RPMI medium  
257 with 10% FCS, penicillin/streptomycin (100 U/ml), and L-Glutamine (2 mM) for 24 hrs. Cell-  
258 free supernatants were collected for measurement of cytokines (stored at -20°C until  
259 required). For dose-dependency response studies, Balb/c bone marrow derived macrophages  
260 (5.0 x 10<sup>5</sup>) were incubated for 30 min with full-length Sm16 (34-117) (5-50 µg/ml) and after  
261 washing in PBS were then stimulated with LPS (10 ng/ml) overnight. Ethical approval for  
262 these studies was granted by the University of Technology Sydney (UTS) Animal Care and  
263 Ethics Committee (Approval Number: 2017-1232) and experiments were conducted in  
264 accordance with the approved guidelines to be compliant with The Australian Code for the  
265 Care and Use of Animals for Scientific Purposes.

266

### 267 **RNA extraction, cDNA synthesis and qPCR**

268 Total RNA was extracted from adult males, adult females, mixed adults, eggs and cercariae  
269 using the miRNeasy Mini Kit (Qiagen, UK) according to the manufacturer's instructions,  
270 eluted in 30 µl RNase-free water. Assessment of RNA concentration and quality was carried  
271 out using the LVis plate functionality on the PolarStar Omega Spectrophotometer (BMG  
272 LabTech, UK). cDNA synthesis was carried out using the High capacity cDNA reverse  
273 transcription kit (ThermoFisher Scientific, UK) according to manufacturer's instructions.

274

275 Quantitative PCR (qPCR) reactions were performed in 20 µl reaction volumes in triplicate,

276 using 1  $\mu$ l cDNA, 10  $\mu$ l of Platinum® SYBR® Green qPCR SuperMix-UDG kit  
277 (ThermoFisher Scientific, UK) and 1  $\mu$ M of each primer to amplify the  
278 Sm16 gene (Sm16\_F 5'-CCGAGTGAAAAAGACATGGAAT-3' and  
279 Sm16\_R 5'-TCAATGCGTCTTCCAAGGAT-3'), and the constitutively expressed *S.*  
280 *mansoni* PAI gene (SmPAI\_F 5'-ACGACCTCGACCAAACATTC-3' and SmPAI\_R 5'-  
281 TAGCTCCGACAGAAGCACCT-3'). qPCR was performed using a Rotor-Gene  
282 thermocycler (Qiagen, UK), with the following cycling conditions: 95°C for 10 s, 50°C for  
283 15 s and 72°C for 20 s. Relative expression analysis was performed manually using Pfaffl's  
284 Augmented  $\Delta\Delta$ Ct method [35], whereby the comparative cycle threshold (Ct) values of the  
285 samples of interest are compared to a control and normalised to the PAI gene expression. The  
286 data are presented relative to the level of Sm16 expression in male adult schistosomes.  
287 Results were analysed using One Way ANOVA (version 6.00 for Windows, GraphPad  
288 Software); P-value <0.05 was deemed statistically significant.

289

#### 290 **Immunolocalization in *S. mansoni* eggs**

291 Paraformaldehyde-fix liver sections were put into embedding cassettes and were dehydrated  
292 in sequential ethanol baths ranging from 50 to 100% with the last two steps in xylene  
293 substitute. Then, tissues were infiltrated with paraffin wax and blocks were placed on a  
294 cooling plate for 15 min to solidify. Five  $\mu$ m sections, cut using a microtome, were floated in  
295 a 45°C water bath and put on slides. Slides were allowed to dry at RT overnight before the  
296 immunolocalization procedure.

297

298 For immunolocalization, slides were put in Safeclear (Xylene substitute; ThermoFisher  
299 Scientific, USA) three times for two minutes. They were subsequently rehydrated by  
300 sequential dipping in ethanol ranging from 100% to 20% with a final step in water. Sections  
301 were treated for two hours at RT in 2% BSA-PBS. They were then incubated overnight at  
302 4°C with rabbit anti-Sm16 (1:100). After three washes of five minutes in PBS, tissues were  
303 incubated for 1 hour with the Alexa Fluor 488-conjugated anti-rabbit (Invitrogen, USA;  
304 1:1000) in 2% BSA-PBS at RT and protected from light. After a wash of five minute in PBS,  
305 DAPI (dilactate; Invitrogen, USA; 1:750 in PBS) was added and incubated for five minutes at  
306 RT. Tissues were washed three times for five minutes with PBS and mounted with  
307 PERMOUNT with a drop of mounting media. Confocal microscopy was performed with a

308 BIO-RAD RADIANCE 2100 confocal laser scanning microscope (CLSM) equipped with a  
309 Nikon E800 fluorescence microscope for confocal image acquisition and the LASERSHARP  
310 2000 software package.

311

### 312 **Internalisation of Sm16 by BMDMs**

313 BMDMs ( $7 \times 10^6$ ) were treated with 10  $\mu\text{g/ml}$  of Alexa Fluor 488-conjugated (Life  
314 Technologies, Vic Australia) recombinant Sm16 or peptide Sm16 (34-117) for 30 min at  
315 37°C then washed and fixed with 4% paraformaldehyde and permeabilized with 0.1% Triton-  
316 X/PBS. Samples were also stained with DAPI for identification of the cell nucleus. To follow  
317 internalisation of Sm16 (34-117), BMDMs ( $7 \times 10^6$ ) were simultaneously incubated with 10  
318  $\mu\text{g/ml}$  of Alexa Fluor 488-labelled Sm16 (34-117) and 60 nM LysoTracker (Life  
319 Technologies, Vic, Australia) and imaged live after 30 min at 37°C as described by Robinson  
320 et al. [36].

321

### 322 **Immunoblot with infected mouse sera**

323 To analyse the proteins by immunoblotting they were first resolved by 12% SDS-PAGE.  
324 Proteins were transferred to nitrocellulose using a semi-dry blotting apparatus. The  
325 nitrocellulose membrane was blocked for 1hr at RT with 15 ml of 5% milk in TBS/0.05%  
326 Tween-20. Then, 15ml of 2.5% milk in TBS/0.05% Tween-20 containing the primary  
327 antibody (anti-Sm16 or serum from infected mice) was added to the nitrocellulose membrane  
328 for 1 hr, with rotation at RT. The nitrocellulose was washed three times for five min each  
329 with TBS/0.05% Tween-20 and then incubated in 15 ml of secondary antibody-peroxidase  
330 conjugate in TBS/0.05%-Tween for 1hr at RT. The nitrocellulose was washed three times for  
331 five min each with TBS/0.05 Tween-20 and then incubated in 15 ml of secondary antibody-  
332 peroxidase conjugate in TBS/0.05%-Tween for 1 hr at RT. The nitrocellulose filter was again  
333 washed three times for five min each. Bound antibody was visualized by adding 1 ml of each  
334 reagent of SuperSignal West Femto Chemiluminescence Substrate (ThermoFisher Scientific,  
335 USA) for 5 minutes. The membrane was dried and developed in the dark using the  
336 autoradiography cassette and Kodak X-OMAT 2000 processor system.

337

### 338 **Cytokine analysis**

339 Human cytokines were measured using human IL-6 uncoated ELISA kit (Invitrogen,

340 ThermoFisher Scientific, UK), human TNF standard ABTS ELISA kit (Peprotech, London,  
341 UK), and human IL-8 ELISA MAX standard kit (Biolegend, San Diego, CA, USA)  
342 according to the manufacturers' instructions. Cytokine arrays used were Human Cytokine  
343 Array C3 (RayBiotech, Norcross, GA, USA). The levels of mouse cytokines present in  
344 culture supernatants were quantified using an ELISA (BD Pharmingen, North Ryde, NSW,  
345 Australia), according to the manufacturer's instructions.

346

### 347 **RNA microarrays**

348 Cells obtained from three independently performed experiments were lysed in 400  $\mu$ l  
349 TRIzol® Reagent (ThermoFisher Scientific, UK) and RNA was purified using PureLink  
350 RNA Mini Kit (ThermoFisher Scientific, UK). RNA integrity number (RIN) scores were  
351 determined using RNA 6000 nano gel matrices (Agilent Technologies, Santa Clara, CA,  
352 USA). Microarray analysis of RNA (100 ng/ $\mu$ l; RIN score  $\geq$  9.9) was carried out using  
353 Human HT-12 v4 BeadChips (Illumina, San Diego, CA, USA). Differential gene expression  
354 analysis was carried out using Partek Genomics Suite (PGS) version 6.6 (Partek  
355 Incorporated, Chesterfield, MO, USA). Genes were filtered for fold change in  $> 1.5$  and  $< -$   
356  $1.5$  and an expression p-value  $< 0.05$ . False discovery rate (FDR) correction was not applied.  
357 The canonical pathway and comparison analyses were generated through the use of  
358 Ingenuity® Pathway Analysis (IPA) (QIAGEN Inc.,  
359 <https://www.qiagenbioinformatics.com/products/ingenuity-pathway-analysis>).

360

### 361 **Statistical analysis**

362 Results were analysed using one-way ANOVAs with Tukey's multiple comparison test.  
363 Differences were not deemed significant when p-values (p)  $> 0.05$ . \*p  $< 0.05$ , \*\*p  $< 0.01$ , \*\*\*p  
364  $< 0.001$ , \*\*\*\*p  $< 0.0001$ .

365

366

## 367 **RESULTS**

### 368 **Schistosome Sm16 is a helminth defence molecule (HDM)**

369 Analysis of genomic data available on WormBase ParaSite facilitated the identification of a  
370 number of homologues of Sm16 and HDMs. Most notably, these molecules were identified

371 solely in the genomes of trematode species (i.e. no HDMs were discovered in the genomes of  
372 any cestode or nematode). Phylogenetic analysis of the HDM sequences recovered from the  
373 various trematode genomes demonstrates a very close relationship between Sm16-like  
374 molecules and *Fasciola*-like HDMs. However, Sm16-like molecules form a distinct branch  
375 and are exclusively produced by organisms of the Schistosomatoidea superfamily, some of  
376 which, for example *S. japonicum*, express several members. We have termed these the  
377 Sm16-like HDMs.

378

379 The *Fasciola*-like HDM branch of the phylogenetic tree (Fig. 1) currently contains HDMs  
380 from *F. hepatica*, *Echinostoma caproni*, *Clonorchis sinensis* and *Opisthorchis viverrini*  
381 which cluster together. It also contains HDMs from various species of the Schistosomatoidea  
382 superfamily; however, these form a separate extended branch. We have termed these the  
383 *Fasciola*-like HDMs.

384

385 **Fig.1. HDMs are a trematode-specific family of immunomodulatory peptides inclusive of Sm16-**  
386 **like molecules.**

387 Midpoint-rooted maximum likelihood phylogram of the trematode-specific HDM family generated by  
388 PhyML, based on the protein sequence Leu<sup>30</sup> to Lys<sup>87</sup> (FhHDM nomenclature) containing the  
389 amphipathic region of the proteins from 12 trematode species: *Clonorchis sinensis* (CsHDM\_1),  
390 *Echinostoma caproni* (EcHDM\_1.1 & EcHDM\_1.2), *Fasciola hepatica* (FhHDM\_1), *Opisthorchis*  
391 *viverrini* (OvHDM\_1), *Schistosoma curassoni* (Sc16 & ScHDM\_2), *S. haematobium* (Sh16 &  
392 ShHDM\_2), *S. japonicum* (Sj16\_1, Sj16\_2, Sj16\_3, SjhHDM\_1 & SjhHDM\_2), *S. mansoni* (Sm16,  
393 SmHDM\_1 & SmHDM\_2), *S. margrebowiei* (Smrz16), *S. matthei* (Smt16), *S. rodhaini* (Sr16,  
394 SrHDM\_1 & SrHDM\_2) and *Trichobilharzia regenti* (Tr16\_1, Tr16\_2 & TrHDM\_2). The clusters of  
395 Sm16-like HDMs and *Fasciola*-like HDMs are shown. Bootstrap support values (1000 iterations) are  
396 shown at each node. Accession number/gene identifiers are presented in S1 Table.

397

398 The evolutionary relationship between members within the Sm16-like HDMs and *Fasciola*-  
399 like HDMs is also supported by their genomic organization; the structure of the genes from  
400 both groups feature four exons separated by three introns of similar lengths. The first exon  
401 encodes the secretory signal peptide. There is a particularly high degree of sequence  
402 conservation in the third and fourth exons across all of the gene sequences that encodes the

403 C-terminal region of the protein which is comprised mainly of  $\alpha$ -helix secondary structure  
404 (S1 Fig, S2 Fig; discussed below).

405

#### 406 **Structural analysis of Sm16 reveals an amphipathic $\alpha$ -helical molecule**

407 Analysis of the amino acid sequence of Sm16 using I-TASSER indicated that much of the  
408 molecule is helical in structure (Fig. 2A and B). This was further confirmed by circular  
409 dichroism analysis of the recombinant Sm16 produced in *Pichia pastoris* (Fig. 2C; S3 Fig.).  
410 Further analysis of the sequence using helical wheel projections (HeliQuest) indicated that  
411 the C-terminal half of Sm16 (residues 52-114) is predominantly uninterrupted amphiphilic  $\alpha$ -  
412 helix containing four hydrophobic hotspots (Fig. 2D). As mentioned above, this C-terminal  
413 section of the protein is highly conserved between the Sm16-like molecules of the  
414 Schistosomatoidea and is encoded by the third and fourth exons of their genes (S1 Fig.).

415

#### 416 **Fig.2. Sm16 predominantly consists of an amphipathic alpha helix.**

417 (A) Predictive secondary structure of Sm16 generated using I-TASSER: H – Helix; S – Strand; C –  
418 coil. Arrow (i) denotes the SignalP 4.1 predicted cleavage site for an N-terminal secretory signal  
419 peptide between residues 22 and 23, and arrow (ii) shows the commencement of the synthetic Sm16  
420 (34-117) peptide sequence. The black line indicates the portion of Sm16 that is amphipathic. (B) 3D  
421 model of full length secreted Sm16, generated using I-TASSER (C) Circular dichroism analysis  
422 performed on recombinant Sm16 in the absence of tetrafluoroethylene (TFE), in 30% TFE, and 60%  
423 TFE. (D) Helical wheel analysis of Sm16 performed using HeliQuest identified four hydrophobic  
424 faces (indicated by blue line through helix) in continuous succession in the amphipathic C-terminal  
425 helix.  $\langle H \rangle$  - Hydrophobicity;  $\langle \mu H \rangle$  - Hydrophobic Moment.

426

#### 427 **Sm16 is expressed predominantly in *S. mansoni* cercariae and eggs**

428 To investigate Sm16 expression in the stages of *S. mansoni* that exist in the mammalian host,  
429 qPCR was performed on mRNA extracted from adults (males, females, and both male and  
430 female mixed), cercariae, and eggs. Sm16 transcription was significantly higher in both *S.*  
431 *mansoni* cercariae and egg samples compared to adult male worms. Low levels of Sm16  
432 expression were observed within the female worms and while higher than in males these  
433 levels were not statistically different (Fig. 3A). Anti-Sm16 antibodies, raised against a  
434 synthetic peptide derived from Sm16 (residues 34-117) was used to probe a Western blot

435 containing *S. mansoni* adults (mixed, males, and females), cercariae, and egg crude extracts.  
436 Sm16 was not detected in the adult worm samples, consistent with the data derived from  
437 qPCR (Fig. 3B). Sm16 was most abundant in cercariae and was detected in eggs when the  
438 immunoblots were exposed for longer periods (see Fig. 3B). Cercariae mechanically-  
439 transformed into schistosomules along with the concentrated transformation medium were  
440 also probed with anti-Sm16 antibodies. This analysis identified Sm16 in both parasite stages  
441 and in the medium demonstrating that Sm16 is released from the cercariae during the  
442 transformation process (Fig. 3C). It is worth noting that mature Sm16 has a lower molecular  
443 weight with reports calculating the mature secreted protein to be between 11.3-11.7 kDa in  
444 size [10,18], but it can run slightly higher on SDS-PAGE

445

446 **Fig 3. Sm16 is expressed in *S. mansoni* cercariae and eggs.**

447 (A) qPCR was used to assess the expression of Sm16 mRNA in *S. mansoni* adults (males, females,  
448 and mixed), cercariae and eggs.  $\Delta\Delta C_t$  values were normalised to the level of PAI expression in  
449 samples (3) and presented as relative to the level of Sm16 expression in male adult schistosomes and  
450 analysed by ANOVA with Tukey's multiple comparison test. \* $p < 0.05$ , \*\* $p < 0.01$ . (B) Western blot  
451 carried out using 5  $\mu\text{g}$  of crude extract from *S. mansoni* adults (mixed, females and males) cercariae  
452 and eggs and probed with an anti-Sm16 antibody. (C) SDS-PAGE analysis (lanes 1-4) and Western  
453 blot (5 -8) of soluble extracts of cercariae (1 and 5), newly-transformed schistosomula (2 and 6),  
454 concentrated transformation medium (3 and 7) and recombinant Sm16 (4 and 8) (D) Blood samples  
455 were taken from mice with experimental schistosomiasis at 0, 5, 10, and 20 weeks post infection and  
456 sera was used to probe Western blots of recombinant Sm16, synthetic peptide Sm16 (34-117), and  
457 recombinant *S. mansoni* cathepsin B1 (SmCB1) (1  $\mu\text{g}$  of each).

458

459 **Sm16 is immunogenic in *S. mansoni*-infected mice, but only late in infection**

460 In order to determine if Sm16 is immunogenic during infection, mice were experimentally  
461 infected with 35 *S. mansoni* cercariae and serum samples harvested at 0-, 5-, 10- and 20-  
462 weeks post-infection were used to probe Western blots containing recombinant Sm16 and  
463 synthetic Sm16 (34-117). Recombinant *S. mansoni* cathepsin B1 (SmCB1), an immunogenic  
464 protease that is produced and secreted abundantly by intra-mammalian *S. mansoni* [37] was  
465 used as a positive control. The immunoblots showed that circulating antibodies to SmCB1 are  
466 present as early as week five post-infection and remain high at week 10 and 20 post-  
467 infection. However, neither recombinant nor synthetic Sm16 preparations were detected on

468 blots that were probed with serum obtained from mice at 5 and 10 weeks after infection but  
469 were strongly reactive with serum taken at 20 weeks post-infection (Fig. 3D).

470

#### 471 **Sm16 is detected in eggs in *S. mansoni*-infected mice**

472 *S. mansoni* eggs were identified in sections of liver tissue from mice that had been  
473 experimentally infected with *S. mansoni* for seven weeks (Fig. 4). Immunofluorescent  
474 imaging by means of probing with anti-Sm16 antibody followed by Alexa Fluor 488-  
475 conjugated anti-rabbit antibodies was used to confirm the presence of Sm16 in *S. mansoni*  
476 eggs. Anti-Sm16 antibody binding was clearly observed within the unembryonated  
477 miracidium in the eggs. No labelling was observed within eggs using control mouse serum.

478

#### 479 **Fig.4. Immunolocalisation of Sm16 in *S. mansoni* eggs**

480 Paraffin was embedded liver sections of *S. mansoni*-infected (7 weeks post-infection) containing *S.*  
481 *mansoni* eggs were probed with anti-Sm16 antibody represented by green fluorescence. For the  
482 negative controls (Ctl) the anti-Sm16 antibodies were first adsorbed with an excess of recombinant  
483 Sm16 prior to being used in the protocol. Nuclear staining was carried out using DAPI represented by  
484 blue fluorescence. The Trans panels shows the sections under light microscopy.

485

#### 486 **Sm16 (34-117) is taken up by macrophages and co-localises with the endo-lysosomes**

487 The *Fasciola*-like HDMs are known to mediate at least a part of their immune modulatory  
488 effect through interaction with macrophages. To determine whether the Sm16 peptides had  
489 the same potential, we visualised the uptake of Alexa Fluor 488-conjugated recombinant  
490 Sm16 and synthetic Sm16 (34-117) by murine macrophages (Fig 5A & B, respectively). Both  
491 recombinant and peptide were clearly internalised by the macrophages, presented as punctate  
492 fluorescence in the cytoplasm fifteen minutes after their addition to cells in culture.  
493 Furthermore, the co-localisation of Sm16 (34-117)-conjugated fluorescence with Lysotracker  
494 indicated that the peptides were located within the endo-lysosomal system of macrophages  
495 (Fig 5C). The labelling with anti-Sm16 appeared more extensive within the  
496 endosomal/lysosomal system than Lysotracker since the latter only fluoresces within the  
497 more acidic mature lysosomes.

498

#### 499 **Fig. 5. Sm16 is internalised by macrophages.**



500 (A) BMDMs ( $7 \times 10^6$ ) were untreated (Un) or incubated with 10  $\mu\text{g/ml}$  Alexa Fluor 488-conjugated  
501 recombinant Sm16 (Sm16) in media for 30 min at 37°C, 5% CO<sub>2</sub>, prior to fixation with 4% PFA.  
502 Samples were also stained with DAPI for identification of the cell nucleus. (B) BMDMs ( $7 \times 10^6$ )  
503 were untreated (Un) or incubated with 10  $\mu\text{g/ml}$  Alexa Fluor 488-conjugated synthetic Sm16 (34-117)  
504 (Sm16) in media for 30 min at 37°C, 5% CO<sub>2</sub>, prior to fixation with 4% PFA. (C) BMDMs ( $7 \times 10^6$ )  
505 were incubated with Alexa 488-conjugated recombinant Sm16 (10 $\mu\text{g/mL}$ ) in media with 60 nM  
506 LysoTracker for 30 min at 37°C, 5% CO<sub>2</sub>. Visual identification of fluorescence in the respective  
507 channels was used to construct the panels; Sm16 staining shown in green, DAPI staining in blue and  
508 LysoTracker staining shown in red. Co-localization identification was confirmed by automated  
509 analysis using the NIS software. Scale bar: 5 $\mu\text{M}$ .

510

### 511 **Sm16 (34-117) affects cytokine production by macrophages**

512 To evaluate the effects of Sm16 (34-117) on the inflammatory responses of human  
513 macrophages, we analyzed supernatants of THP-1 macrophages treated with Sm16 (34-117)  
514 and LPS using a broad cytokine array (S3 Table). The data showed that Sm16 (34-117) alone  
515 increased secretion of cytokines including IL-6, IL-1 $\beta$ , GM-CSF, I-309, TNF, and IL-10.  
516 Stimulation with LPS alone also increased secretion of these cytokines; however, the  
517 quantities of IL-6, GM-CSF, TNF were higher than in the macrophages stimulated by Sm16  
518 (34-117) while induction of IL-1 $\beta$  and I-309 were lower and IL-10 the same. Therefore, both  
519 Sm16 and LPS induce a pro-inflammatory response from THP-1 macrophages, albeit with  
520 some differences. However, addition of Sm16 (34-117) to THP-1 cells alongside LPS  
521 suppressed the induction of the LPS-induced inflammatory response in macrophages (S3  
522 Table).

523

524 To further validate these observations, we measured IL-6 and TNF by ELISA in supernatants  
525 of THP-1 macrophages treated with Sm16 (34-117) alone, LPS alone and both together. Cells  
526 treated with Sm16 (34-117) alone did not secrete TNF but did secrete higher levels of IL-6  
527 compared to untreated controls, although this increase was not statistically significant (Fig.  
528 6A). This weak pro-inflammatory effect of Sm16 (34-117) was also observed using BMDMs  
529 from C57/BL6 and Balb/c mice (data not shown). By contrast, LPS stimulation elicited a  
530 highly significant increase in levels of IL-6 and TNF secreted by THP-1 macrophages.  
531 Addition of Sm16 (34-117) to LPS-treated cells significantly reduced the amount of IL-6 and  
532 TNF released (Fig. 6A).

533

534 **Fig. 6. Effects of synthetic peptide Sm16 (34-117) treatment on cytokine secretion by**  
535 **macrophages.**

536 (A) IL-6 and TNF in cell supernatants of THP-1 macrophages ( $2.5 \times 10^5$ ) treated with Sm16 (34-117)  
537 (20  $\mu\text{g/ml}$ ), LPS (100 ng/ml) and Sm16 (34-117) + LPS for 16 hrs were quantified by ELISA. Data  
538 derived from three independently performed experiments was analysed using repeated measures  
539 ANOVA with Tukey's multiple comparison test. (B) Sm16 (34-117) inhibits macrophage activation  
540 in a dose-dependent manner. Bone marrow derived macrophages ( $5.0 \times 10^5$ ) from Balb/c mice were  
541 incubated for 30 min with full-length Sm16 (34-117) (5-50  $\mu\text{g/ml}$ ) and after washing in PBS were  
542 then stimulated with LPS (10 ng/ml) 16h. TNF and IL6 in cell supernatants was measured by ELISA.  
543 (C-D) Effect of Sm16 (34-117) and small peptides derivatives from the C-terminal amphipathic helix.  
544 THP-1 cells were treated with 20  $\mu\text{g/ml}$  of Sm16 (52-77), Sm16 (60-80), Sm16 (73-107), Sm16 (85-  
545 96), Sm16 (85-115), or Sm16 (95-115) in the absence (C) and presence (D) of LPS stimulation (100  
546 ng/ml). IL6 in cell supernatants was measured by ELISA. Data analysed by ANOVA with Tukey's  
547 multiple comparison test as above. \* $p < 0.05$ , \*\* $p < 0.01$ , \*\*\* $p < 0.001$ .

548

549 Studies were performed with BMDMs from Balb/c mice to demonstrate that the effect of  
550 Sm16 was not restricted to THP-1 cells. In addition, to exclude the possibility of the anti-  
551 inflammatory effects of Sm16 (34-117) resulting from its direct binding to LPS (especially at  
552 high doses) we incubated BMDMs with Sm16 (34-117) at a range of concentrations (5-50  
553  $\mu\text{g}$ ) for 30 min before washing the cells and subsequently adding LPS. Cell supernatants were  
554 collected following an overnight incubation and the quantities of TNF and IL6 in samples  
555 were measured by ELISA (Fig. 6B). Sm16 (34-117) inhibited macrophage activation in a  
556 dose-dependent manner (5 - 50  $\mu\text{g/ml}$ ). Our data shows, therefore, that Sm16 can effectively  
557 modulate the inflammatory response of these murine macrophages and human THP-1 cells to  
558 stimulation with LPS.

559

560 To determine if the conserved  $\alpha$ -helix region held the immune modulating activity of Sm16  
561 and to identify a smaller effective anti-inflammatory peptide, we synthesised peptides  
562 corresponding to the following residues, Sm16 (52-77), Sm16 (60-80), Sm16 (73-107), Sm16  
563 (85-96), Sm16 (85-115), or Sm16 (95-115), and tested these against THP-1 cells. We used  
564 IL-6 as our measure of blocking activity since microarray data showed that this cytokine was  
565 affected to a greater degree by Sm16 (52-77) than TNF (fold change of 309 vs 14.9, S3) and  
566 its secretion from LPS-stimulated THP-1 cells was effectively blocked by Sm16 (52-77) (Fig.

567 6A). Compared to the parent Sm16 (34-117), none of these peptide derivatives significantly  
568 induced IL-6 secretion directly from THP-1 macrophages (Fig. 6C). Moreover, no peptide  
569 significantly blocked the pro-inflammatory effect of LPS (Fig. 6D).

570

### 571 **Changes to human macrophage gene expression exerted by Sm16 (34-117)**

572 To investigate the effects of Sm16 (34-117) on human macrophage gene transcription, THP-1  
573 macrophages were incubated with Sm16 (34-117), LPS, or LPS and Sm16 (34-117) and  
574 mRNA transcripts analysed using Illumina HT12 V.4 Expression Bead Chips. In cells treated  
575 with Sm16 (34-117) only, transcription of a total of 1217 genes was significantly ( $p < 0.05$ )  
576 changed: 751 gene transcripts exhibited increased expression ( $> 1.5$  fold) and 466 were down-  
577 regulated ( $< -1.5$  fold) (Fig. 7A; see S4 Table for top 70 genes differentially regulated by  
578 Sm16). LPS treatment significantly affected the transcription of 1855 genes, 486 of which  
579 showed increased expression while 1369 decreased (Fig. 7A).

580

### 581 **Fig. 7. Sm16 (34-117) treatment significantly alters gene expression in THP-1 macrophages.**

582 THP-1 macrophages ( $2.5 \times 10^5$ ) were treated with Sm16 (34-117) (20  $\mu\text{g/ml}$ ) and/or LPS (100  $\text{ng/ml}$ )  
583 or not treated (Untreated) for 4 hrs before extracting RNA for analysis using Illumina HT12 V.4  
584 Expression Bead Chips. Significantly ( $p < 0.05$ ) differentially expressed genes were identified by  
585 ANOVA when analysing Sm16 vs Untreated; LPS vs Untreated; Sm16 + LPS vs LPS alone. Data is  
586 derived from three independently performed experiments. (A) Overview of differential gene  
587 expression analyses detailing total number of genes that were up- and down-regulated  $> 1.5$  fold and  
588  $< -1.5$  fold, represented by orange and blue bars, respectively. (B) Venn diagram depicting overlap of  
589 differentially expressed genes across the respective analyses. (C) Canonical pathways predicted to be  
590 affected by the respective treatments as determined by IPA analysis of the differentially expressed  
591 genes ( $\pm 1.5$  fold change). Inhibition and activation of pathways are shown by the z-score, represented  
592 by a scale of blue to orange, respectively.

593

594 Of the 1217 genes for which expression was changed significantly by Sm16 (34-117), 65%  
595 (795) overlapped with the genes significantly changed by LPS stimulation. The directionality  
596 of the genes in this cohort was identical across the two sets of differential gene expression  
597 analyses, i.e. the same genes were up- or down-regulated in each group. Analysis of the  
598 remaining 35% (422) of genes that exclusively responded to Sm16 (34-117) revealed that  
599 these genes are most highly associated with cellular movement and development,

600 inflammatory responses and tissue morphology. Based on their differential expression, IPA  
601 indicates that Sm16 is likely to cause an increase in lymphocyte populations, increase cell  
602 viability, cellular movement and phagocytosis, as well as a decrease in myeloid cell  
603 populations and inflammatory responses (S4 Fig.).

604

605 THP-1 macrophages treated with LPS and Sm16 (34-117) showed transcriptional changes in  
606 only 106 genes compared to cells treated with LPS alone: of these, 37 genes showed >1.5  
607 fold increased expression, while 69 <-1.5 fold decreased in expression (Fig. 7A and C; see  
608 also S5 Table for top 70 genes differentially regulated by LPS followed by Sm16). A full list  
609 of the differential expression analyses results can be found in S6 Table.

610

611 Based on the differential changes to gene expression, Ingenuity Pathway Analysis (IPA)  
612 predicted that the pathways most negatively affected by treatment of the macrophages with  
613 either Sm16 (34-117) or LPS are nuclear receptors PPAR and LXR/RXR. These transcription  
614 factors are intricately involved in regulating cellular metabolism of macrophages (fatty acid,  
615 cholesterol and glucose homeostasis) and are central to the modulation of innate immune cell  
616 fate [38,39] (Fig. 7C). However, when cells were first treated with LPS and then followed by  
617 Sm16 (34-117) both of these signaling pathways were up-regulated (Fig. 7C). Conversely,  
618 several inflammatory signaling pathways including dendritic cell maturation, NF- $\kappa$ B  
619 signaling, HMGB1 signaling, acute phase responses, and IL-6 are putatively activated by  
620 Sm16 (34-117) and LPS alone, and are inhibited when cells are first treated with LPS and  
621 then with Sm16 (34-117) (Fig. 7C).

622

623 The predicted implications of the changes to gene expression exerted by Sm16 (34-117)  
624 alone on the biological processes of macrophages include increased leukocyte activation and  
625 adhesion, chemotaxis, inflammatory responses and cell and organismal survival (S5 Fig.).  
626 Sm16 (34-117), however, showed differences with LPS most obviously in its suppression of  
627 biological functions associated with morbidity/mortality and organismal death that were  
628 activated by LPS. These results further emphasise that while the Sm16 (34-117) itself can  
629 activate various inflammatory responses in macrophages it also has potent inhibitory activity  
630 against LPS-induced inflammation.

631

632 **DISCUSSION**

633 Phylogenetic, structural and functional analysis of the well-known schistosome-secreted  
634 molecule, Sm16, provides strong evidence for its inclusion within the helminth defence  
635 molecule (HDM) family of immunomodulators. Previously, our clustal analysis of several  
636 members of HDMs suggested an evolutionary link between Sm16 and HDMs [40]. Given the  
637 extensive range of genomic data now available for helminth species, a more thorough  
638 phylogenetic analysis was carried out and confirmed these previous findings. Gene structure  
639 analysis further supported the expansion of this family of Sm16-like molecules by  
640 demonstrating a conserved intron-exon pattern amongst the HDM and Sm16 genes.

641

642 Furthermore, we found that Sm16-like HDMs form a distinct branch of the HDMs specific to  
643 the Schistosomatoidea superfamily which is consistent with the early evolutionary divergence  
644 of this superfamily from the other trematode families [41]. Sequence alignments of Sm16  
645 homologues in *S. japonicum*, *S. haematobium*, *S. curassoni*, *S. margrebowiei*, *S. mattheei*, *S.*  
646 *rodhaini*, and *Trichobilharzia regenti*, showed that Sm16-like molecules are structurally  
647 highly conserved within this superfamily. Since the Schistosomatoidea superfamily also  
648 express members of the Fasciola-like HDMs it is clear that the two branches arose from a  
649 common ancestral HDM. Therefore, these analyses verify the view that the Sm16-like HDMs  
650 diverged to perform a function(s) that is unique to Schistosomatoidea, most obviously, a role  
651 in the process of skin invasion by cercariae which is unique to this trematode superfamily.

652

653 Looking more broadly, our genomic searches also discovered that the HDM family of  
654 molecules are exclusively present in the genomes of trematode species. All trematode  
655 genomes examined possessed at least one HDM-encoding gene whereas these were absent  
656 from all nematode and cestode genomes. Such conservation within trematode species  
657 indicates that HDM molecules are of great importance to the development and/or survival of  
658 these digenean endoparasites. Our studies with *F. hepatica* (FhHDM/FhMF6p) have  
659 suggested that trematodes secrete HDMs to modulate the host immune responses to ensure  
660 their longevity, possibly by preventing the activation of pro-inflammatory responses via the  
661 inflammasome [42]. Another idea proposed by Martinez-Sernandez et al. [43] relates to the  
662 heme-binding property of FhHDM/FhMF6p and suggests that they play a role in the

663 scavenging of potentially damaging free heme released from haemoglobin during feeding by  
664 the parasites.

665

666 Structural analysis of the Sm16 protein demonstrates that it is primarily an  $\alpha$ -helical  
667 molecule. We highlighted the presence of four consecutive hydrophobic faces in the major  $\alpha$ -  
668 helical region that spans much of the Sm16 C-terminal section (residues 52-115).  
669 Hydrophobic residues were concentrated on one face of each  $\alpha$ -helix and indicate that Sm16  
670 is considerably amphipathic. This shows that the structural and biochemical properties of the  
671 Sm16-like and Fasciola-like HDMs are also very similar in that they are  $\alpha$ -helical,  
672 amphipathic, and cationic [24]. Indeed, the integrity of the C-terminal sequence and structure  
673 of these molecules appears to be inherently important for their immunomodulatory activity.  
674 Truncation or disruption of the Sm16 sequence at the C-terminus impairs its ability to bind to  
675 surface membranes and to be internalised by mammalian cells [14,20,44], which has also  
676 been observed in our studies on *F. hepatica* FhHDM/FhMF6p [36].

677

678 The first studies of Sm16 two decades ago found that it was expressed exclusively by  
679 sporocysts, cercariae, and early schistosomulae of *S. mansoni* [9,10]. We also found that  
680 Sm16 constitutes a considerable proportion of the proteins in cercariae and, in keeping with  
681 the proteomic studies by Curwen et al. [45], is secreted during the mechanical transformation  
682 of cercariae to schistosomulae. The molecule is stored in abundance within the acetabular  
683 glands and rapidly expelled from these during skin penetration [45,46]; however, this  
684 transient expression and secretion into the host tissues is clearly insufficient to induce  
685 detectable antibodies in the early weeks following a primary infection. Most reports agree  
686 that Sm16 is not expressed by adult worms [9–12,46]. Although we detected low levels of  
687 Sm16 expression in female adult and mixed-adult extracts by qPCR in this study, we presume  
688 that this is due to some residual presence of eggs in adult female worms as no expression was  
689 found in male worms.

690

691 Our finding that Sm16 is expressed in eggs disagrees with most earlier studies and the more  
692 recent report by Bernardes et al. [12]. The discrepancy may be because we employed more  
693 sensitive methods of Western blots (chemiluminescence) and gene amplification by qPCR.  
694 This would also explain why our results are consistent with studies by Gobert et al. [11] who

695 showed using microarrays that *S. japonicum* Sj16 is enriched in eggs. Our  
696 immunohistochemistry studies also clearly showed the presence of Sm16 within the  
697 unembryonated miracidium. This raises the possibility that Sm16 is involved in egg-driven  
698 immunomodulation and while we did not observe Sm16 in the tissues surrounding the egg,  
699 the presence of a signal peptide in the molecule and antibodies to Sm16 in the blood of  
700 infected mice suggests that it is secreted. Although antibodies were not detected until  
701 sometime after week 10 post-infection this could be because the molecule is secreted in low  
702 levels, is poorly immunogenic due to its small size, or is secreted late in the entrapped egg.  
703 Also, there may be little or no response to Sm16 until the host immune system is exposed to  
704 the increasing number of eggs released by females or when tissue-lodged eggs die and  
705 degrade and their contents disperse into the tissues. Nevertheless, our studies encourage  
706 future investigations to determine if Sm16 plays a role in egg-induced inflammation, in  
707 down-modulating the egg granuloma (which occurs between 8 – 20 weeks after infection)  
708 and/or in facilitating the immune-dependent exit of eggs through the intestine [47].

709

710 Much of the research to date that has evaluated the function of Sm16 has been conducted  
711 using a recombinant formulation expressed in *E. coli* that either features a mutation with two  
712 alanine substitutions at positions 92 and 93 [13,14,44] or a truncation of the last 27 C-  
713 terminal residues [12]. These modifications were made due to the inability to express soluble  
714 recombinant Sm16 in this prokaryotic system, perhaps owing to the amphipathic nature of the  
715 C-terminal section of the protein. However, we would argue that these modifications also  
716 compromised the native structure of the molecule and, more importantly, its immunological  
717 function since these alterations were made within the region that is critical for the  
718 immunomodulatory activity of HDM. Indeed, Robinson et al. [36] demonstrated that  
719 disruption of the C-terminal amphipathic  $\alpha$ -helical by substitution of a leucine for a proline  
720 resulted in its inability to bind lipid membranes and inhibit vacuolar ATPase. We report here  
721 that full-length Sm16 can be expressed and secreted in the eukaryotic methylotrophic yeast *P.*  
722 *pastoris* and that this recombinant, as well as a synthetic version, bound to macrophages and  
723 was endocytosed into the endosomal/lysosomal system like other HDMs [36]. Bernardes et  
724 al. [12] acknowledged that the failure of their recombinant Sm16 vaccine to promote parasite  
725 elimination could have been because it lacked the C-terminal 27 residues; therefore, a repeat  
726 of these trials with yeast-expressed or synthetic full-length Sm16 may be worthwhile.

727

728 Another anomaly we found between our studies and previously reported work regards the  
729 sequence identities between the Sm16 of *S. mansoni* and the homologs found in *S.*  
730 *japonicum*. In the report of the discovery of the Sj16 homolog in *S. japonicum*, Hu et al. [18]  
731 states that this molecule ‘shares 99% identity with Sm16 in its nucleotide sequence, and  
732 100% identity in its protein sequence’. A recombinant formulation of the molecule was  
733 produced, termed rSj16, and has been used in a number of studies [18-23, 48-52]. We show  
734 here with our in-depth analysis of the genomic data currently available that while Sm16  
735 represents a single copy gene in *S. mansoni*, three Sm16-like molecules exist in the genome  
736 of *S. japonicum*; however, none of the three Sj16s share 100% primary sequence identity  
737 with Sm16. The percentage identities of Sj16\_1, Sj16\_2 and Sj16\_3 compared to Sm16 are  
738 66%, 63% and 38%, respectively.

739

740 We opted to evaluate the bioactive properties of a chemically synthesized Sm16 as we have  
741 previously shown that HDMs bind LPS very strongly in solutions making it difficult to  
742 isolate them free of endotoxin [24]. The LPS-binding capacity of HDM have also been  
743 reported by Martinez-Sernandez et al. [43,53] and Kang et al. [54]. Chemically synthesized  
744 peptides have various production benefits compared to recombinantly-produced peptides  
745 including reduced costs, capacity to up-scale, increased purity, and are endotoxin free. Here  
746 we show that Sm16 (34-117) is readily internalized by the endocytic/lysosomal system of  
747 macrophages and causes significant changes to the transcription of genes that are primarily  
748 associated with immune responses. Macrophages are key players in the innate immune  
749 response to pathogens and are also pivotal in coordinating tissue repair [55,56]. In the early  
750 stages of infection innate immune responses are potently stimulated by schistosomes and  
751 typically a Th1-type inflammatory response is mounted by the host [6]. In light of our  
752 observations that Sm16 exhibits weak pro-inflammatory activity, these responses could be  
753 associated in part with the early and rapid release of an abundance of this molecule. Upon  
754 infection, schistosome larvae induce IL-12p40 secretion from dendritic cells and  
755 macrophages, a cytokine considered to be a key mediator of the cutaneous inflammation [57].  
756 Furthermore, radiation-attenuated cercariae, which have a delayed migration through the  
757 skin, elicit an IL-12p40-mediated Th1 response that confers protection against further  
758 parasite invasion [58]. The treatment of macrophages with Sm16 (34-117) resulted in a 1.5-  
759 fold increase ( $p= 0.03$ ) in IL-12p40 transcripts (IL12B; S6 Table) which would support the  
760 idea that Sm16 secreted by schistosomulae during infection could contribute to the IL-12p40-



761 mediated inflammatory response. In addition, it has been suggested that IL-12p40 also has  
762 the propensity to inhibit eosinophilia [59], which may facilitate unimpeded access for the  
763 worm into host vasculature. This weak but significant pro-inflammatory property of Sm16-  
764 like HDMs has been previously overlooked in studies of its immunomodulatory activity as  
765 experiments involving macrophages treated with Sm16 alone were not performed or reported  
766 [14,18].

767

768 Sm16 (34-117) attenuated the pro-inflammatory responses of LPS-stimulated macrophages  
769 compared to LPS controls in a dose-dependent manner. This observation suggested that  
770 Sm16 (34-117) exposure arrests macrophage responses to TLR4 activation and is supported  
771 by the anti-inflammatory activity of Sm16-derived molecules, and other HDMs, in  
772 dampening responses to LPS [13,14,17,19,20,22,24,26,40,50-52]. Our results also confirm  
773 that the chemically synthesized Sm16 (34-117) retains the anti-inflammatory properties of  
774 Sm16 (and also binds anti-Sm16 antibodies in infected mice blood). However, an attempt to  
775 identify a shorter peptide sequence with similar activity to the parent molecule activity, albeit  
776 focused around the  $\alpha$ -helical hotspots in the C-terminal region, was not successful and  
777 suggests that the intrinsic property of the Sm16 to be taken up by cells and alter their  
778 transcriptional profile is dependent on several conjoined motifs. However, in light of the  
779 immunotherapeutic potential of Sm16, we have established that the synthetic Sm16 (34-117)  
780 is bioactive and can be used in future studies to elucidate Sm16 function as well as being a  
781 cost-effective option for further bio-therapeutics development.

782

783 Analysis of cytokine production by human acute monocytic leukaemia THP-1 macrophages  
784 stimulated with Sm16 and with LPS showed that both induced pro-inflammatory responses,  
785 although the latter exhibit far higher potency. Microarray analysis of these cells found that of  
786 the 1217 genes that showed a significant change in expression when stimulated with Sm16  
787 (34-117), 65% (795) overlapped with the genes also significantly changed by LPS  
788 stimulation, with comparable up or down expression of genes. However, Sm16 exclusively  
789 altered the expression of 422 genes (35%) that were most highly associated with cellular  
790 movement and development, inflammatory responses and tissue morphology, and according  
791 to Ingenuity Pathway Analysis (IPA) were likely to elicit an increase in lymphocyte  
792 populations, increase cell viability, cellular movement and phagocytosis, in addition to

793 decreasing myeloid cell populations and inflammatory responses. The data therefore indicates  
794 that while Sm16 (34-117) displays pro-inflammatory activity with similarities to LPS its  
795 effect on macrophage cell activation and signalling was distinct.

796

797 Interrogation of the RNA microarray data of Sm16 (34-117)-treated THP-1 macrophages  
798 suggested that at least one mechanism utilised by Sm16 to regulate the response of  
799 macrophages to activation by inflammatory ligands (such as LPS) was via the control of  
800 ligand-activated transcription factors PPAR and LXR. These nuclear receptors compete to  
801 hetero-dimerise with RXR before binding to DNA response elements in the promoter regions  
802 of target genes that control macrophage lipid, cholesterol and glucose homeostasis [38,39].  
803 PPAR/LXR are expressed by a wide range of hematopoietic immune cells, including  
804 macrophages, and are known to have immunosuppressive effects on both the innate and  
805 adaptive arms of the mammalian immune response. They can alter gene expression to inhibit  
806 inflammatory cytokine transcription and the development of CD4+ T cells, and have also  
807 been linked to parasite-mediated immune modulation [60]. In this study, PPAR/LXR  
808 signaling was activated when the human macrophages were treated with the combination of  
809 LPS and Sm16 (34-117) which could suggest that this is a mechanism through which the  
810 peptide exerts its anti-inflammatory effects. Interestingly, using microarrays, Tanaka et al.  
811 [26] recently showed that blocking of LPS-induced inflammatory responses in murine  
812 (Balb/c) bone-marrow derived macrophages by a synthetic *F. hepatica* HDM also involved in  
813 the activation of PPAR/LXR signaling. *In vivo* experiments performed by Wang et al. [23]  
814 showed that rSj16 delivery protected mice from DSS-induced colitis which correlated with  
815 the inhibition of PPAR- $\alpha$  signaling in the colon. Therefore, further investigation into the  
816 intricacies of Sm16 control of PPAR/LXR signaling, the implications of its effects on  
817 inflammatory responses, and indeed the affected cell-types that orchestrate the  
818 immunomodulation *in vivo* is warranted.

819

820 The secretion of antigens by helminth parasites may inhibit endotoxin-induced inflammation  
821 to dampen Th1-type responses and indirectly promote a Th2 environment in which  
822 endoparasitic helminths can thrive [61–63]. However, the immune system  
823 modulation/polarisation exerted by flatworms and other helminth infections can leave hosts  
824 more susceptible to secondary infections that could potentially be deleterious for both the

825 host and parasite [64–66]. We have suggested that dampening classical immune activation by  
826 endotoxin with secreted molecules could be a mechanism employed by trematodes like *F.*  
827 *hepatica* and *S. mansoni* to confer tolerance to secondary bacterial infections [67]. A feature  
828 of these infections is the disruption of anatomical barriers, either at the skin, intestine, bladder  
829 or bile ducts which could lead to the translocation of bacteria into the host circulation and  
830 cause septicaemia and septic shock. Indeed, a study has shown that systemic endotoxin levels  
831 in individuals with schistosomiasis were extremely high, notably higher than lethal endotoxin  
832 levels reported in cases of septic shock [68]. Accordingly, secretion of HDM by these  
833 flatworms may be important in sustaining a general dampening of pro-inflammatory  
834 responses to co-infection with microbial pathogens, possibly via activation of PPAR and  
835 LXR/RXR transcription factors.

836

837 In conclusion, we have shown that Sm16 and its homologues within the Schistosomatoidea  
838 superfamily are distinct members of the HDM family of short secretory peptides that are  
839 expressed exclusively by trematode species. Thus, our studies elevate the general importance  
840 of HDMs as a *bone fide* family of immunomodulatory molecules in these globally important  
841 parasites of humans and their livestock. In the context of the collective published data, our  
842 study broadens our understanding of Sm16-like molecules and supports the idea that they  
843 play an important role in key host-parasite interactions including the  
844 scavenging/detoxification of haemoglobin-derived heme and iron transport [43,53] while also  
845 advancing the proposal that the secretion of Sm16 by eggs could contribute to disease  
846 pathogenesis and/or transmission. However, further research, for example through specific  
847 gene knock-down and/or gene editing, would go a long way towards elucidating the true  
848 importance of Sm16 in schistosomiasis. Finally, as we have shown that a synthetic form of  
849 this molecule, Sm16 (34-117), retains bioactive and immunomodulatory properties which  
850 augers well for the future pursuit of cost-effective trematode-derived immune-therapeutics.

851

852

### 853 **ACKNOWLEDGMENTS**

854 JS was supported by a fellowship provided by the Department for the Economy through  
855 Queen's University Belfast, Northern Ireland, UK. KT, SC, BGS and JPD were supported by  
856 a Canadian Institute of Health Research (CIHR) Chair (Tier 1) in Infectious Diseases

857 awarded to JPD. KC and JPD were funded by the Science Foundation Ireland (SFI, Republic  
858 of Ireland) Research Professorship grant 17/RP/5368. RA, JT and SD was supported by an  
859 NH&MRC project grant APP1142006. CCT and SW are supported by the Medical Research  
860 Council, UK. The funders had no role in study design, data collection and analysis, decision  
861 to publish, or preparation of the manuscript.

862

### 863 **AUTHOR CONTRIBUTIONS**

864 J.S: Conceptualization, Formal analysis, Investigation, Methodology, Visualization, Writing  
865 – original draft, Writing – review & editing

866 K.C: Conceptualization, Formal analysis, Investigation, Methodology, Visualization, Writing  
867 – original draft, Writing – review & editing

868 R.A: Conceptualization, Formal Analysis, Investigation, Methodology, Visualization

869 K.T: Conceptualization, Formal Analysis, Methodology, Visualization

870 S.C: Conceptualization, Formal Analysis, Methodology, Visualization

871 B.G.S: Conceptualization, Formal Analysis, Methodology, Visualization

872 J.T: Conceptualization, Formal Analysis, Investigation, Methodology, Visualization

873 S.D: Conceptualization, Formal analysis, Funding acquisition, Investigation, Methodology,  
874 Resources, Supervision, Writing – original draft, Writing – review & editing

875 C.C.T: Conceptualization, Formal analysis, Funding acquisition, Investigation, Methodology,  
876 Resources, Supervision, Writing – original draft, Writing – review & editing

877 S.W: Conceptualization, Formal analysis, Funding acquisition, Investigation, Methodology,  
878 Resources, Supervision, Writing – original draft, Writing – review & editing

879 J.P.D: Conceptualization, Formal analysis, Funding acquisition, Investigation, Methodology,  
880 Resources, Supervision, Writing – original draft, Writing – review & editing

881

882

### 883 **REFERENCES**

884 1. Abajobir AA, Abate KH, Abbafati C, Abbas KM, Abd-Allah F, Abdulkader RS, et al.  
885 Global, regional, and national incidence, prevalence, and years lived with disability for  
886 328 diseases and injuries for 195 countries, 1990–2016: a systematic analysis for the  
887 Global Burden of Disease Study 2016. *Lancet*. 2017;390: 1211–1259.  
888 doi:10.1016/S0140-6736(17)32154-2

889 2. Freer JB, Bourke CD, Durhuus GH, Kjetland EF, Prendergast AJ. Schistosomiasis in

- 890 the first 1000 days. *Lancet Infect Dis.* 2017;3099. doi:10.1016/S1473-3099(17)30490-  
891 5
- 892 3. Jenkins SJ, Hewitson JP, Jenkins GR, Mountford P. Modulation of the host's  
893 immune response by schistosome larvae. *Parasite Immunol.* 2005;27: 385–393.  
894 doi:10.1111/j.1365-3024.2005.00789.x.Modulation
- 895 4. Fairfax K, Nascimento M, Huang SCC, Everts B, Pearce EJ. Th2 responses in  
896 schistosomiasis. *Semin Immunopathol.* 2012;34: 863–871. doi:10.1007/s00281-012-  
897 0354-4
- 898 5. Colley DG, Bustinduy AL, Secor WE, King CH. Human schistosomiasis. *Lancet.*  
899 2014;383: 2253–2264. doi:10.1016/S0140-6736(13)61949-2
- 900 6. Lundy SK, Lukacs NW. Chronic schistosome infection leads to modulation of  
901 granuloma formation and systemic immune suppression. *Front Immunol.* 2013;4: 1–  
902 18. doi:10.3389/fimmu.2013.00039
- 903 7. Hams E, Aviello G, Fallon PG. The *Schistosoma* granuloma: Friend or foe? *Front*  
904 *Immunol.* 2013;4: 1–8. doi:10.3389/fimmu.2013.00089
- 905 8. Colley DG, Secor WE. Immunology of human schistosomiasis. *Parasite Immunol.*  
906 2014;36: 347–357. doi:10.1111/pim.12087
- 907 9. Ram D, Lantner F, Ziv E, Lardans V, Schechter I. Cloning of the SmSPO-1 gene  
908 preferentially expressed in sporocyst during the life cycle of the parasitic helminth  
909 *Schistosoma mansoni*. *Biochim Biophys Acta - Mol Basis Dis.* 1999;1453: 412–416.  
910 doi:10.1016/S0925-4439(99)00012-5
- 911 10. Valle C, Festucci A, Calogero A, Macrì P, Mecozzi B, Liberti P, et al. Stage-specific  
912 expression of a *Schistosoma mansoni* polypeptide similar to the vertebrate regulatory  
913 protein stathmin. *J Biol Chem.* 1999;274: 33869–74. doi:10.1074/JBC.274.48.33869
- 914 11. Gobert GN, Moertel L, Brindley PJ, McManus DP. Developmental gene expression  
915 profiles of the human pathogen *Schistosoma japonicum*. *BMC Genomics.* 2009;10.  
916 doi:10.1186/1471-2164-10-128
- 917 12. Bernardes WP de OS, de Araújo JM, Carvalho GB, Alves CC, de Moura Coelho AT,  
918 Dutra ITS, et al. Sm16, A *Schistosoma mansoni* Immunomodulatory Protein, Fails to  
919 Elicit a Protective Immune Response and Does Not Have an Essential Role in Parasite  
920 Survival in the Definitive Host. *J Immunol Res.* 2019;2019: 1–16.

- 921 doi:10.1155/2019/6793596
- 922 13. Brännström K, Sellin ME, Holmfeldt P, Brattsand M, Gullberg M. The *Schistosoma*  
923 *mansoni* protein Sm16/SmSLP/SmSPO-1 assembles into a nine-subunit oligomer with  
924 potential to inhibit Toll-like receptor signaling. *Infect Immun*. 2009;77: 1144–54.  
925 doi:10.1128/IAI.01126-08
- 926 14. Sanin DE, Mountford AP. Sm16, a major component of *Schistosoma mansoni*  
927 cercarial excretory/secretory products, prevents macrophage classical activation and  
928 delays antigen processing. *Parasites and Vectors*. 2015;8: 1. doi:10.1186/s13071-014-  
929 0608-1
- 930 15. Ramaswamy K, Salafsky B, Potluri S, He YX, Li JW, Shibuya T. Secretion of an anti-  
931 inflammatory, immunomodulatory factor by Schistosomulae of *Schistosoma mansoni*.  
932 *J Inflamm* 1996; 46: 13-22.
- 933 16. Rao KV, Ramaswamy K. Cloning and expression of a gene encoding Sm16, an anti-  
934 inflammatory protein from *Schistosoma mansoni*. *Mol Biochem Parasitol*. 2000;  
935 108:101-8. doi:10.1016/s0166-6851(00)00206-7
- 936 17. Rao KVN, He Y-X, Ramaswamy K. Suppression of cutaneous inflammation by  
937 intradermal gene delivery. *Gene Ther*. 2002;9: 38–45. doi:10.1038/sj.gt.3301622
- 938 18. Hu S, Wu Z, Yang L, Fung MC. Molecular cloning and expression of a functional  
939 anti-inflammatory protein, Sj16, of *Schistosoma japonicum*. *Int J Parasitol*. 2009;39:  
940 191–200. doi:10.1016/j.ijpara.2008.06.017
- 941 19. Sun XJ, Li R, Sun, Zhou Y, Wang Y, Liu XJ, et al. Unique roles of *Schistosoma*  
942 *japonicum* protein Sj16 to induce IFN-gamma and IL-10 producing CD4+CD25+  
943 regulatory T cells in vitro and in vivo. *Parasite Immunol*. 2012; 430–9.  
944 doi:10.1111/j.1365-3024.2012.01377.x
- 945 20. Sun X, Yang F, Shen J, Liu Z, Liang J, Zheng H, et al. Recombinant Sj16 from  
946 *Schistosoma japonicum* contains a functional N-terminal nuclear localization signal  
947 necessary for nuclear translocation in dendritic cells and interleukin-10 production.  
948 *Parasitol Res*. 2016;115: 4559–4571. doi:10.1007/s00436-016-5247-3
- 949 21. Sun X, Lv ZY, Peng H, Fung MQ, Yang L, Yang J, et al. Effects of a recombinant  
950 schistosomal-derived anti-inflammatory molecular (rSj16) on the lipopolysaccharide  
951 (LPS)-induced activated RAW264.7. *Parasitol Res*. 2012;110: 2429–2437.

- 952 doi:10.1007/s00436-011-2782-9
- 953 22. Sun X, Liu YH, Lv ZY, Yang LL, Hu SM, Zheng HQ, et al. rSj16, a recombinant  
954 protein of *Schistosoma japonicum*-derived molecule, reduces severity of the complete  
955 Freund's adjuvant-induced adjuvant arthritis in rats' model. *Parasite Immunol.*  
956 2010;32: 739–748. doi:10.1111/j.1365-3024.2010.01240.x
- 957 23. Wang L, Xie H, Xu L, Liao Q, Wan S, Yu Z, et al. rSj16 protects against DSS-induced  
958 colitis by inhibiting the PPAR- $\alpha$  signaling pathway. *Theranostics.* 2017;7: 3446–3460.  
959 doi:10.7150/thno.20359
- 960 24. Thivierge K, Cotton S, Schaefer DA, Riggs MW, To J, Lund ME, et al. Cathelicidin-  
961 like helminth defence molecules (HDMs): absence of cytotoxic, anti-microbial and  
962 anti-protozoan activities imply a specific adaptation to immune modulation. *PLoS*  
963 *Negl Trop Dis.* 2013;7: e2307. doi:10.1371/journal.pntd.0002307
- 964 25. Lund ME, Greer J, Dixit A, Alvarado R, Mccauley-Winter P, To J, et al. A parasite-  
965 derived 68-mer peptide ameliorates autoimmune disease in murine models of Type 1  
966 diabetes and multiple sclerosis. *Sci Rep.* 2016;6. doi:10.1038/srep37789
- 967 26. Tanaka A, Allam VSRR, Simpson J, Tiberti N, Shiels J, To J, et al. The Parasitic 68-  
968 mer Peptide FhHDM-1 inhibits mixed granulocytic inflammation and airway  
969 hyperreactivity in experimental asthma. *J Allergy Clin Immunol.* 2018; 2–5.  
970 doi:10.1016/j.jaci.2018.01.050
- 971 27. Dalton JP, Day SR, Drew AC, Brindley PJ. A method for the isolation of schistosome  
972 eggs and miracidia free of contaminating host tissues. *Parasitology.* 1997;115: 29–32.  
973 doi:10.1017/S0031182097001091
- 974 28. Collins PR, Stack CM, O'Neill SM, Doyle S, Ryan T, Brennan GP et al. Cathepsin L1,  
975 the major protease involved in liver fluke (*Fasciola hepatica*) virulence: propeptide  
976 cleavage sites and autoactivation of the zymogen secreted from gastrodermal cells. *J.*  
977 *Biol. Chem.* 279, 17038-17046 (2004). doi:10.1074/jbc.M308831200
- 978 29. Stack CM, Dalton JP, Cunneen M, Donnelly S. De-glycosylation of *Pichia pastoris*-  
979 produced *Schistosoma mansoni* cathepsin B eliminates non-specific reactivity with  
980 IgG in normal human serum. *J Immunol Methods.* 2005;304: 151–157.  
981 doi:10.1016/j.jim.2005.07.019
- 982 30. Katoh K, Standley DM. MAFFT Multiple Sequence Alignment Software Version 7:

- 983 Improvements in Performance and Usability. *Mol Biol Evol.* 2013;30: 772–780.  
984 doi:10.1093/molbev/mst010
- 985 31. Guindon S, Dufayard J-F, Lefort V, Anisimova M, Hordijk W, Gascuel O. New  
986 Algorithms and Methods to Estimate Maximum-Likelihood Phylogenies: Assessing  
987 the Performance of PhyML 3.0. *Syst Biol.* 2010;59: 307–321.  
988 doi:10.1093/sysbio/syq010
- 989 32. Petersen TN, Brunak S, Von Heijne G, Nielsen H. SignalP 4.0: Discriminating signal  
990 peptides from transmembrane regions. *Nat Methods.* 2011;8: 785–786.  
991 doi:10.1038/nmeth.1701
- 992 33. Yang J, Zhang Y. I-TASSER server: New development for protein structure and  
993 function predictions. *Nucleic Acids Res.* 2015;43: W174–W181.  
994 doi:10.1093/nar/gkv342
- 995 34. Gautier R, Douguet D, Antony B, Drin G. HELIQUEST: A web server to screen  
996 sequences with specific  $\alpha$ -helical properties. *Bioinformatics.* 2008;24: 2101–2102.  
997 doi:10.1093/bioinformatics/btn392
- 998 35. Pfaffl MW. A new mathematical model for relative quantification in real-time RT–  
999 PCR. *Nucleic Acids Res.* 2001;29: e45. doi:10.1093/NAR/29.9.E45
- 1000 36. Robinson MW, Alvarado R, To J, Hutchinson AT, Dowdell SN, Lund M, et al. A  
1001 helminth cathelicidin-like protein suppresses antigen processing and presentation in  
1002 macrophages via inhibition of lysosomal vATPase. *FASEB J.* 2012;26: 4614–4627.  
1003 doi:10.1096/fj.12-213876
- 1004 37. Soloviova K, Fox EC, Dalton JP, Caffrey CR, Davies SJ. A secreted schistosome  
1005 cathepsin B1 cysteine protease and acute schistosome infection induce a transient T  
1006 helper 17 response. Correa-Oliveira R, editor. *PLoS Negl Trop Dis.* 2019;13:  
1007 e0007070. doi:10.1371/journal.pntd.0007070
- 1008 38. Rigamonti E, Chinetti-Gbaguidi G, Staels B. Regulation of macrophage functions by  
1009 PPAR-alpha, PPAR-gamma, and LXRs in mice and men. *Arterioscler Thromb Vasc*  
1010 *Biol.* 2008;28: 1050–9. doi:10.1161/ATVBAHA.107.158998
- 1011 39. Leopold Wager CM, Arnett E, Schlesinger LS. Macrophage nuclear receptors:  
1012 Emerging key players in infectious diseases. Bliska JB, editor. *PLOS Pathog.* 2019;15:  
1013 e1007585. doi:10.1371/journal.ppat.1007585



- 1014 40. Robinson MW, Donnelly S, Hutchinson AT, To J, Taylor NL, Norton RS, et al. A  
1015 family of helminth molecules that modulate innate cell responses via molecular  
1016 mimicry of host antimicrobial peptides. *PLoS Pathog.* 2011;7: e1002042.  
1017 doi:10.1371/journal.ppat.1002042
- 1018 41. Cribb TH, Bray RA, Littlewood DT. The nature and evolution of the association  
1019 among digeneans, molluscs and fishes. *Int J Parasitol.* 2001;31: 997–1011.  
1020 doi:10.1016/s0020-7519(01)00204-1
- 1021 42. Alvarado R, To J, Lund ME, Pinar A, Mansell A, Robinson MW, et al. The immune  
1022 modulatory peptide FhHDM-1 secreted by the helminth *Fasciola hepatica* prevents  
1023 NLRP3 inflammasome activation by inhibiting endolysosomal acidification in  
1024 macrophages. *FASEB J.* 2017;31: 85–95. doi:10.1096/fj.201500093r
- 1025 43. Martínez-Sernández V, Mezo M, González-Warleta M, Perteguer MJ, Gárate T,  
1026 Romarís F, et al. Delineating distinct heme-scavenging and -binding functions of  
1027 domains in MF6p/helminth defense molecule (HDM) proteins from parasitic  
1028 flatworms. *J Biol Chem.* 2017;292: 8667–8682. doi:10.1074/jbc.M116.771675
- 1029 44. Holmfeldt P, Brännström K, Sellin ME, Segerman B, Carlsson SR, Gullberg M. The  
1030 *Schistosoma mansoni* protein Sm16/SmSLP/SmSPO-1 is a membrane-binding protein  
1031 that lacks the proposed microtubule-regulatory activity. *Mol Biochem Parasitol.*  
1032 2007;156: 225–234. doi:10.1016/j.molbiopara.2007.08.006
- 1033 45. Curwen RS, Ashton PD, Sundaralingam S, Wilson RA. Identification of Novel  
1034 Proteases and Immunomodulators in the Secretions of Schistosome Cercariae That  
1035 Facilitate Host Entry. *Mol Cell Proteomics.* 2006;5: 835–844.  
1036 doi:10.1074/mcp.M500313-MCP200
- 1037 46. Paveley RA, Aynsley SA, Cook PC, Turner JD, Mountford AP. Fluorescent Imaging  
1038 of Antigen Released by a Skin-Invading Helminth Reveals Differential Uptake and  
1039 Activation Profiles by Antigen Presenting Cells. Jones MK, editor. *PLoS Negl Trop*  
1040 *Dis.* 2009;3: e528. doi:10.1371/journal.pntd.0000528
- 1041 47. Schwartz C, Fallon PG. *Schistosoma* “Eggs-Itting” the Host: Granuloma Formation and  
1042 Egg Excretion. *Front Immunol.* 2018;9: 2492. doi:10.3389/FIMMU.2018.02492
- 1043 48. Sun X, Zhou H-J, Lv Z-Y, Zhang S-M, Hu S-M, Zheng H-Q, et al. Studies on  
1044 immunomodulation effect of recombinant Sj16 from *Schistosoma japonicum* on

- 1045 inflammation response of host. Chinese J Parasitol Parasit Dis. 2008;26: 113–8.
- 1046 49. Hu S, Yang L, Wu Z, Mak NK, Leung KN, Fung MC. Anti-inflammatory protein of  
1047 *Schistosoma japonicum* directs the differentiation of the WEHI-3B JCS cells and  
1048 mouse bone marrow cells to macrophages. J Biomed Biotechnol. 2010;2010: 867368.  
1049 doi:10.1155/2010/867368
- 1050 50. Hu S, Yang L, Wu Z, Wong CS, Fung MC. Suppression of Adaptive Immunity to  
1051 Heterologous Antigens by SJ16 of *Schistosoma japonicum*. J Parasitol. 2012;98: 274–  
1052 283. doi:10.1645/GE-2692.1
- 1053 51. Shen J, Xu L, Liu Z, Li N, Wang L, Lv Z, et al. Gene expression profile of LPS-  
1054 stimulated dendritic cells induced by a recombinant Sj16 (rSj16) derived from  
1055 *Schistosoma japonicum*. Parasitol Res. 2014;113: 3073–3083. doi:10.1007/s00436-  
1056 014-3973-y
- 1057 52. Shen J, Wang L, Peng M, Liu Z, Zhang B, Zhou T, et al. Recombinant Sj16 protein  
1058 with novel activity alleviates hepatic granulomatous inflammation and fibrosis induced  
1059 by *Schistosoma japonicum* associated with M2 macrophages in a mouse model.  
1060 Parasites and Vectors. 2019;12: 1–15. doi:10.1186/s13071-019-3697-z
- 1061 53. Martínez-Sernández V, Mezo M, González-Warleta M, Perteguer MJ, Muiño L,  
1062 Guitián E, et al. The MF6p/FhHDM-1 major antigen secreted by the trematode  
1063 parasite *Fasciola hepatica* is a heme-binding protein. J Biol Chem. 2014;289: 1441–  
1064 56. doi:10.1074/jbc.M113.499517
- 1065 54. Kang J-M, Yoo WG, Lê HG, Lee J, Sohn W-M, Na B-K. Clonorchis sinensis  
1066 MF6p/HDM (CsMF6p/HDM) induces pro-inflammatory immune response in RAW  
1067 264.7 macrophage cells via NF-κB-dependent MAPK pathways. Parasit Vectors.  
1068 2020;13: 20. doi:10.1186/s13071-020-3882-0
- 1069 55. Faz-Lopez B, Morales-Montor J, Terrazas LI. Role of Macrophages in the Repair  
1070 Process during the Tissue Migrating and Resident Helminth Infections. Biomed Res  
1071 Int. 2016;2016. doi:10.1155/2016/8634603
- 1072 56. Wynn TA, Vannella KM. Macrophages in tissue repair, regeneration, and fibrosis.  
1073 Immunity. 2017;44: 450–462. doi:10.1016/j.immuni.2016.02.015.Macrophages
- 1074 57. Hogg KG, Kumkate S, Anderson S, Mountford AP. Interleukin-12 p40 secretion by  
1075 cutaneous CD11c+ and F4/80+ cells is a major feature of the innate immune response

- 1076 in mice that develop Th1-mediated protective immunity to *Schistosoma mansoni*.  
1077 Infect Immun. 2003;71: 3563–71. doi:10.1128/IAI.71.6.3563
- 1078 58. Hogg KG, Kumkate S, Mountford AP. IL-10 regulates early IL-12-mediated immune  
1079 responses induced by the radiation-attenuated schistosome vaccine. Int Immunol.  
1080 2003;15: 1451–1459. doi:10.1093/intimm/dxg142
- 1081 59. Lee YL, Fu CL, Chiang BL. Administration of interleukin-12 exerts a therapeutic  
1082 instead of a long- term preventive effect on mite Der p I allergen-induced animal  
1083 model of airway inflammation. Immunology. 1999;97: 232–240. doi:10.1046/j.1365-  
1084 2567.1999.00768.x
- 1085 60. Chan MM, Evans KW, Moore AR, Fong D. Peroxisome Proliferator-Activated  
1086 Receptor (PPAR): Balance for survival in parasitic infections. J Biomed Biotechnol.  
1087 2010. doi:10.1155/2010/828951
- 1088 61. Allen JE, Wynn TA. Evolution of Th2 Immunity: A Rapid Repair Response to Tissue  
1089 Destructive Pathogens. Madhani HD, editor. PLoS Pathog. 2011;7: e1002003.  
1090 doi:10.1371/journal.ppat.1002003
- 1091 62. Girgis NM, Gundra UM, Loke P. Immune Regulation during Helminth Infections.  
1092 Knoll LJ, editor. PLoS Pathog. 2013;9: e1003250. doi:10.1371/journal.ppat.1003250
- 1093 63. Gazzinelli-Guimaraes PH, Nutman TB. Helminth parasites and immune regulation.  
1094 F1000Research. 2018;7: 1–12. doi:10.12688/F1000RESEARCH.15596.1
- 1095 64. Potian JA, Rafi W, Bhatt K, McBride A, Gause WC, Salgame P. Preexisting helminth  
1096 infection induces inhibition of innate pulmonary anti-tuberculosis defense by engaging  
1097 the IL-4 receptor pathway. J Exp Med. 2011;208: 1863–1874.  
1098 doi:10.1084/jem.20091473
- 1099 65. Monin L, Griffiths KL, Lam WY, Gopal R, Kang DD, Ahmed M, et al. Helminth-  
1100 induced arginase-1 exacerbates lung inflammation and disease severity in tuberculosis.  
1101 J Clin Invest. 2015;125: 4699–713. doi:10.1172/JCI77378
- 1102 66. Schramm G, Suwandi A, Galeev A, Sharma S, Braun J, Claes A-K, et al. Schistosome  
1103 Eggs Impair Protective Th1/Th17 Immune Responses Against Salmonella Infection.  
1104 Front Immunol. 2018;9: 2614. doi:10.3389/fimmu.2018.02614
- 1105 67. Robinson MW, Donnelly S, Dalton JP. Helminth defence molecules-  
1106 immunomodulators designed by parasites! Front Microbiol. 2013;4: 1–4.

1107 doi:10.3389/fmicb.2013.00296

1108 68. Onguru D, Liang Y, Griffith Q, Nikolajczyk B, Mwinzi P, Ganley-Leal L. Short  
1109 report: Human schistosomiasis is associated with endotoxemia and toll-like receptor 2-  
1110 and 4-bearing B cells. *Am J Trop Med Hyg.* 2011;84: 321–324.

1111 doi:10.4269/ajtmh.2011.10-0397

1112

## 1113 SUPPORTING INFORMATION

### 1114 **S1 Fig. Structural analyses of the Schistosomatidae-specific family of Sm16-like**

1115 **molecules. (A)** A MAFFT amino acid alignment of the Sm16-like proteins from trematodes.

1116 The predicted signal peptide is shown underlined and in italics. The black line depicts the  
1117 area of the Sm16-like molecules that is amphipathic. The four colour blocks represent the  
1118 sequence encoded by the four exons depicted in the genomic organisation below. **(B)**

1119 Schematic representation of the genomic organisation of the Sm16-like molecules. Exons and

1120 introns are represented as coloured boxes and lines, respectively. The numbers denote the

1121 number of nucleotide base pairs. ^Sr16 gene – Part of the last exon is missing due to an error

1122 in the *Schistosoma rodhaini* genome scaffold. \*Sh16 gene – The second intron cannot be

1123 determined within the current *Schistosoma haematobium* genome assembly; currently the

1124 first two exons are present on the forward DNA strand, with the remaining part of the gene

1125 present on the opposite strand of the scaffold. ±As the Sj16\_2 and Tr16\_2 genes are present

1126 at the beginning of their respective scaffolds the first exon cannot be determined within the

1127 current genome assemblies.

1128

### 1129 **S2 Fig. Structural analyses of the Trematode-specific family of Fasciola-like HDM**

1130 **molecules. (A)** A MAFFT amino acid alignment of the Fasciola-like HDM proteins. The

1131 predicted signal peptide is shown underlined and in italics. The four colour blocks represent

1132 the sequence encoded by the four exons depicted in the genomic organisation below. **(B)**

1133 Schematic representation of the genomic organisation of the Fasciola-like HDM molecules.

1134 Exons and introns are represented as coloured boxes and lines, respectively. The numbers

1135 denote the number of nucleotide base pairs. ^As the TrHDM gene is present at the beginning

1136 of the genomic scaffold the first exon cannot be determined within the current genome

1137 assemblies.

1138

1139 **S3 Fig. Purification of yeast-expressed recombinant Sm16.** Top: gene accession numbers  
1140 of Sm16/SPO-1 and primary sequence. The signal sequence is shaded in black. The DNA  
1141 sequence encoding Sm16 without the signal sequence was cloned into a pPink $\alpha$ -HC vector  
1142 and expressed in *Pichia pastoris* as a secreted 6xHis-tagged protein. Recombinant Sm16 was  
1143 purified using Ni<sup>2+</sup>-affinity chromatography and analysed on a 16% SDS-PAGE  
1144 electrophoresis gel which was subsequently stained with Coomassie blue. Sm16 was also  
1145 detected using anti-His tag and anti-Sm16 antibodies.

1146

1147 **S4 Fig. Biological processes associated with genes independently affected by Sm16.** IPA  
1148 of 422 genes differentially up-regulated >1.5 fold ( $p < 0.05$ ) in macrophages by treatment  
1149 with Sm16 and independent of genes associated with the cellular response to LPS,  
1150 represented as log p value. The orange line highlights the threshold of  $-\log(0.05) / 1.3$ .

1151

1152 **S5 Fig. Comparative analyses of the biological effects exerted by Sm16 (34-117) and**  
1153 **LPS as shown by differential gene expression.** THP-1 macrophages ( $2.5 \times 10^5$ ) were  
1154 untreated or treated with Sm16 (34-117) alone (20  $\mu\text{g/ml}$ ), LPS alone (100  $\text{ng/ml}$ ) or with  
1155 both Sm16 (34-117) and LPS for 4 hrs before extracting RNA for analysis using Illumina  
1156 HT12 V.4 Expression Bead Chips. Significantly differentially expressed genes were  
1157 identified by ANOVA and IPA analysis of these produced predicted effects on associated  
1158 functions. Inhibition and activation of pathways are shown by the z-score, represented by a  
1159 scale of blue to orange, respectively.

1160

1161 **S1 Table. Accession number/protein identifiers of the sequences used for the**  
1162 **phylogenetic analysis.**

1163

1164 **S2 Table: Details of parasite genome databases and seed sequences used for BLAST**  
1165 **analysis**

1166

1167 **S3 Table. Cytokine array analysis of supernatants of THP-1 macrophages that were**  
1168 **untreated or treated with Sm16 (34-117), LPS or LPS and Sm16 (34-117).** Numbers  
1169 represent fold change in cytokine signal. Signal intensity was measured by densitometry.  
1170 When comparing separate membranes values were normalised using a comparative ratio  
1171 calculated using densitometry values for membrane positive control spots.

1172

1173 **S4 Table: Top 70 genes differentially regulated by adding Sm16 to THP-1 macrophages.**

1174

1175 **S5 Table: Top 70 genes differentially regulated by adding Sm16 to LPS-treated THP-1**

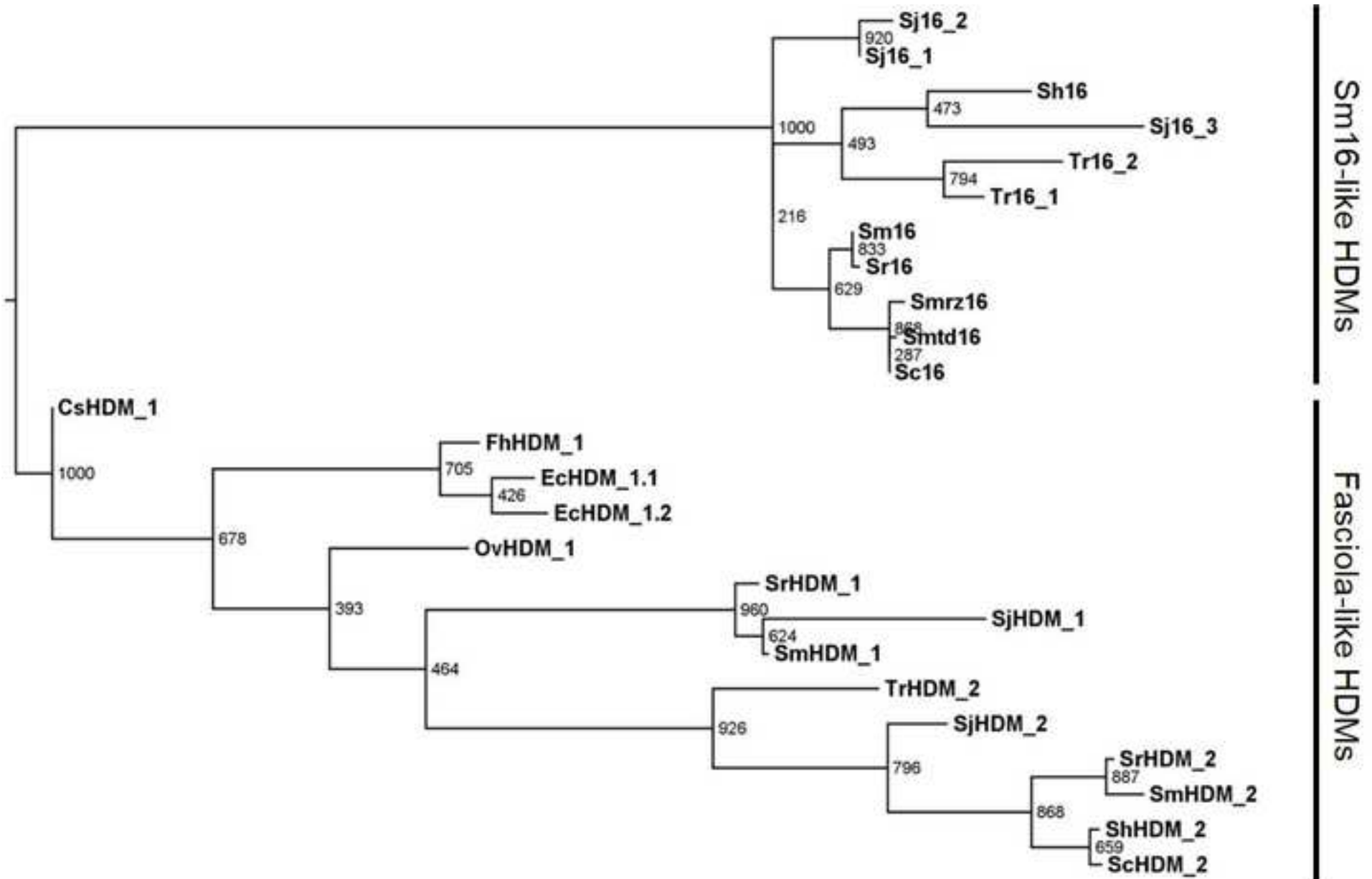
1176 **macrophages.**

1177

1178 **S6 Table: Differential expression analyses by microarray of THP-1 macrophages**

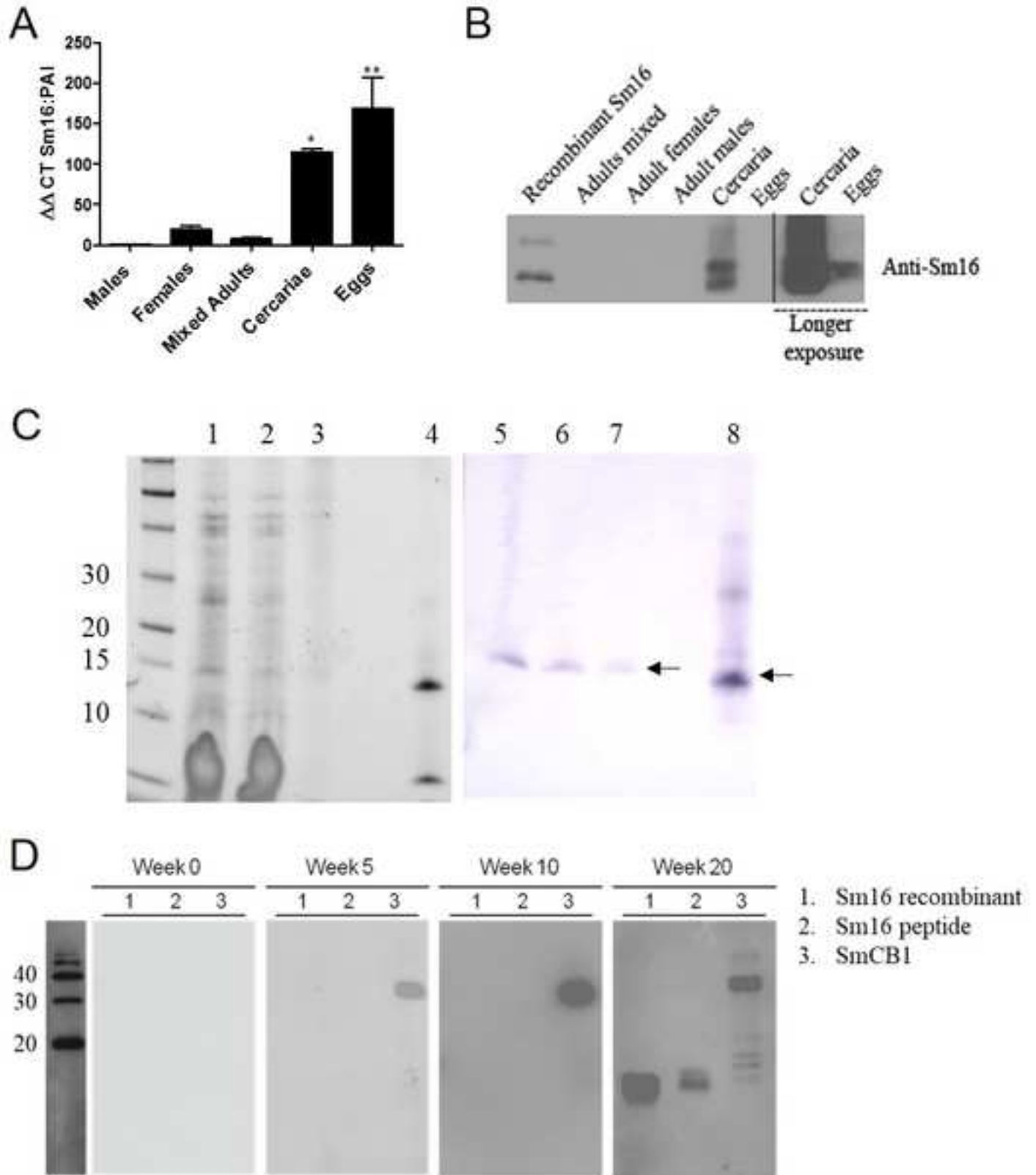
1179 **treated with Sm16 and LPS.**

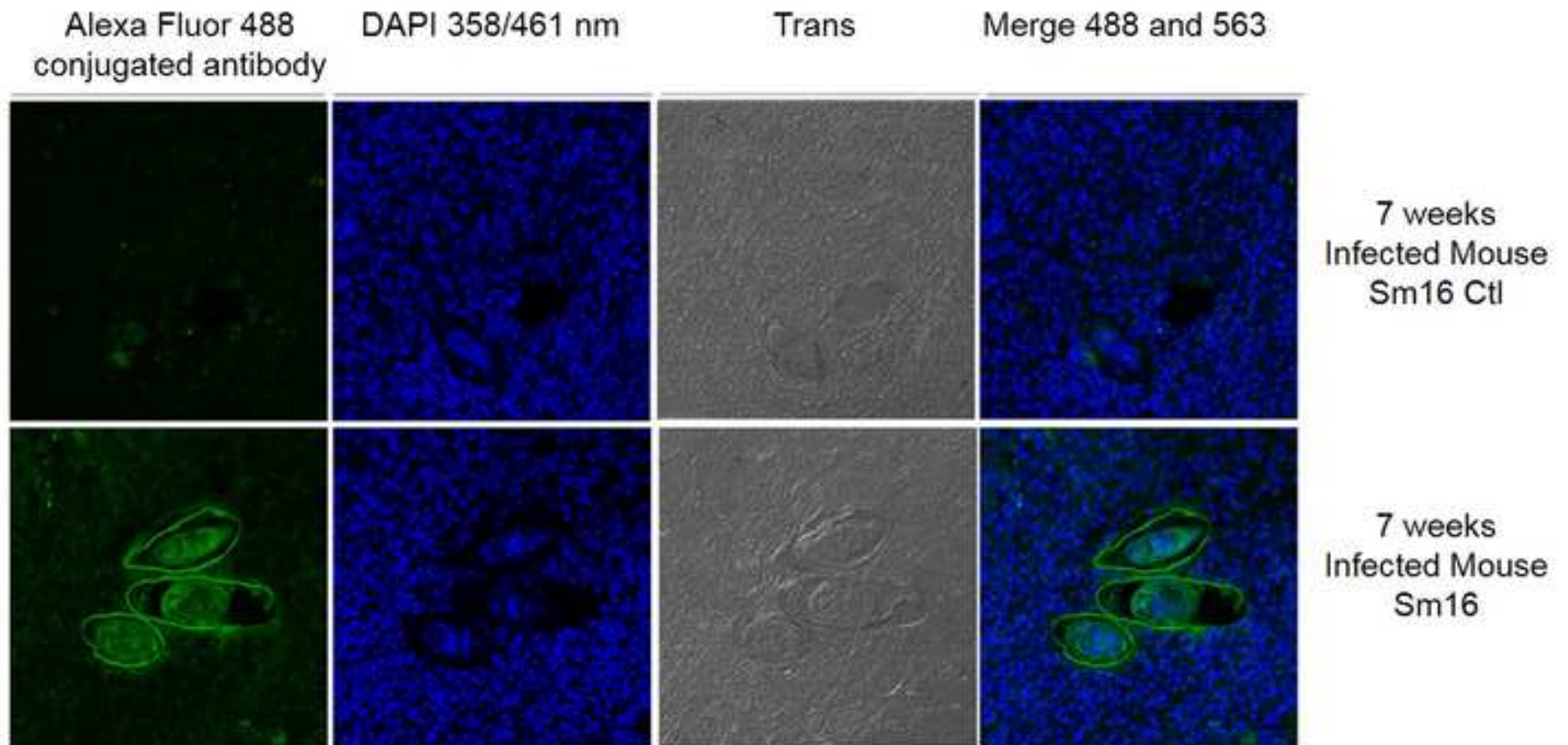
1180

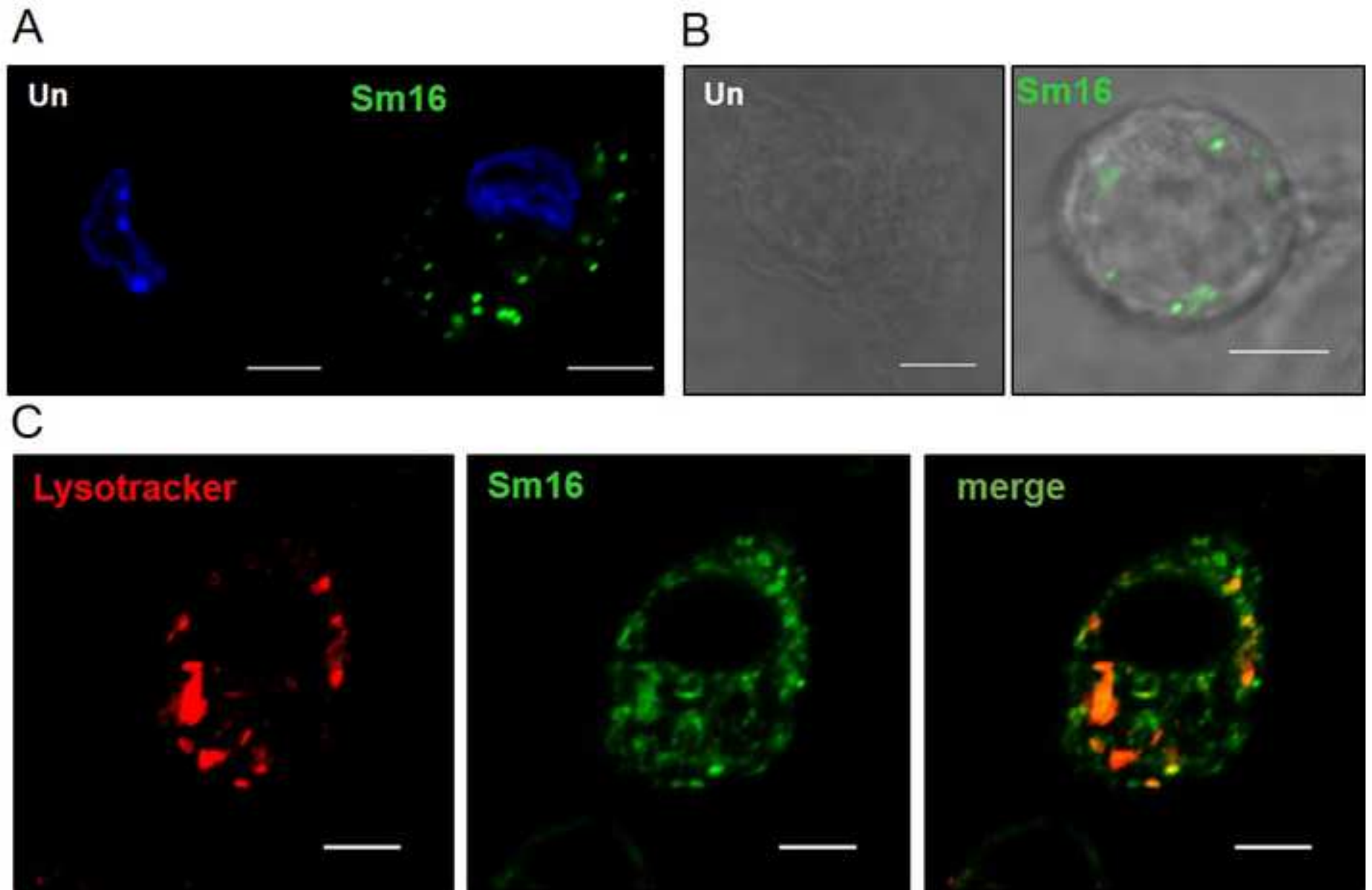


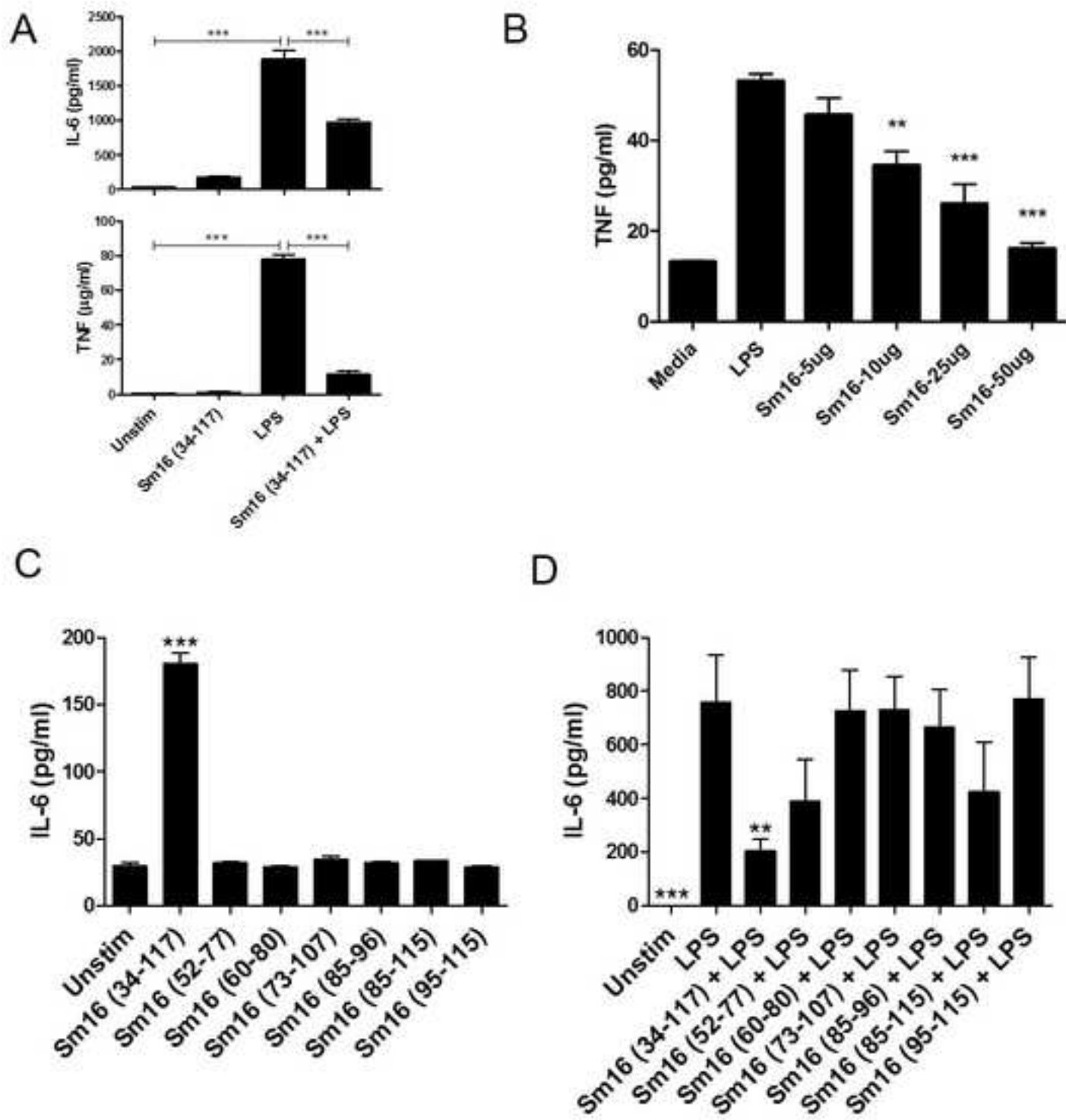


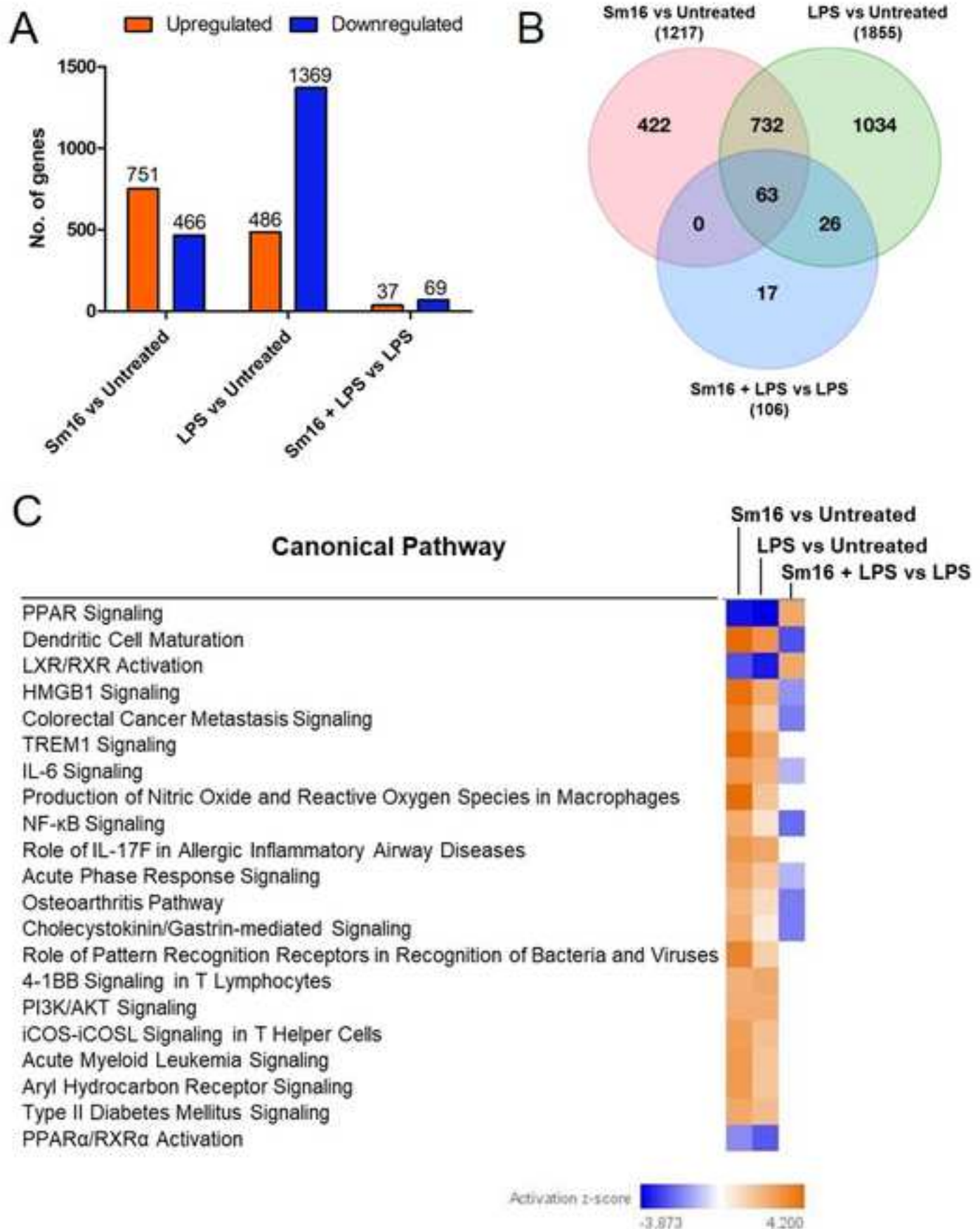


























Click here to access/download  
**Supporting Information**  
Supplemental Information V3.docx





Click here to access/download  
**Supporting Information**  
S6 Table.xlsx